



Original Research

Exogenous-organic-matter-driven mobilization of groundwater arsenic



Fan Feng^{a, b, c}, Yonghai Jiang^{a, b}, Yongfeng Jia^{a, b, *}, Xinying Lian^{a, b}, Changjian Shang^{a, b}, Meng Zhao^{a, b}

^a State Key Laboratory of Environmental Criteria and Risk Assessment, Chinese Research Academy of Environmental Sciences, Beijing, 100012, China

^b State Environmental Protection Key Laboratory of Simulation and Control of Groundwater Pollution, Chinese Research Academy of Environmental Sciences, Beijing, 100012, China

^c College of Water Sciences, Beijing Normal University, Beijing, 100875, China

ARTICLE INFO

Article history:

Received 20 September 2022

Received in revised form

21 January 2023

Accepted 24 January 2023

Keywords:

Groundwater arsenic

Exogenous organic matter

Redox condition

Secondary pollution risk

ABSTRACT

The potential release capacity of arsenic (As) from sediment was evaluated under a high level of exogenous organic matter (EOM) with both bioreactive and chemically reactive organic matters (OMs). The OMs were characterized by FI, HIX, BIX, and SUVA₂₅₄ fluorescence indices showing the biological activities were kept at a high level during the experimental period. At the genus level, Fe/Mn/As-reducing bacteria (*Geobacter*, *Pseudomonas*, *Bacillus*, and *Clostridium*) and bacteria (*Paenibacillus*, *Acidovorax*, *Delftia*, and *Sphingomonas*) that can participate in metabolic transformation using EOM were identified. The reducing condition occurs which promoted As, Fe, and Mn releases at very high concentrations of OM. However, As release increased during the first 15–20 days, followed by a decline contributed by secondary iron precipitation. The degree of As release may be limited by the reactivity of Fe (hydro)oxides. The EOM infiltration enhances As and Mn releases in aqueous conditions causing the risk of groundwater pollution, which could occur in specific sites such as landfills, petrochemical sites, and managed aquifer recharge projects.

© 2023 The Authors. Published by Elsevier B.V. on behalf of Chinese Society for Environmental Sciences, Harbin Institute of Technology, Chinese Research Academy of Environmental Sciences. This is an open access article under the CC BY-NC-ND license (<http://creativecommons.org/licenses/by-nc-nd/4.0/>).

1. Introduction

High arsenic (As) groundwater is considered an important and difficult issue in the field of hydrogeology and environmental geology due to its toxicity and widespread distribution globally [1–3]. A notable feature of groundwater with high levels of As is its high degree of inhomogeneity, with As concentrations ranging from drinking water standards to hundreds of $\mu\text{g L}^{-1}$ in different wells located only a few meters apart in the same village [4–7]. Researchers have offered various explanations for such huge differences in As concentration distribution but still do not fully understand this phenomenon. For example, the reactivities of Fe–Mn oxides/hydroxides and organic matters [8,9], the source of groundwater recharge [10–12], microbial processes [13–16],

groundwater major components [17–19] and groundwater flow rates [20] are all important factors affecting As spatial distribution. The most important factor is its significant redox sensitivity, and any change in redox conditions may cause changes in its concentration [16,21]. This causes problems in the explanation of its enrichment as well as potential anthropogenic impacts on its deteriorating contamination.

Arsenic undergoes dynamic biogeochemical processes such as desorption, reduction, complexation, and co-precipitation [22]. These processes are usually controlled by the interaction between Fe (hydro)oxides and organic matters (OMs), especially dissolved organic matter (DOM) [23,24]. The OM can bind to metals through strong adsorption, ion exchange, competition, and chelation [25], resulting in the transformation and mobilization of As from the sediments into the water. OM can be used as a catalyst for mobilizing As via metal chelation under anaerobic conditions [26]. The OM not only serves as a substrate for microbial metabolism but also as an electron acceptor and donor or an electron shuttle to promote the transport and transformation of As [27,28]. As can also react

* Corresponding author. State Key Laboratory of Environmental Criteria and Risk Assessment Chinese Research Academy of Environmental Sciences, Beijing, 100012, China.

E-mail address: jiayf@craes.org.cn (Y. Jia).

with carboxyl/phenol groups in DOC to form ternary complexes with Fe and As. The mobility of As is regulated by free (uncomplexed) dissolved As, As–Fe–DOM colloids, and dissolved complexes [29].

The reductive dissolution of As-bound Fe–Mn oxides/hydroxides is thought to be the most important reason for groundwater As contamination worldwide [30]. Iron reduction and the associated release of As are attributed to the microbial dissimilatory reduction processes [11,31–34]. As a heterotrophic process, it must be combined with the oxidation of an energy source, most commonly OM. DOM is a mixture of polyphasic organic molecules commonly found in aquatic ecosystems [35], which is divided into refractory DOM, such as humic acid (HA) and xanthate acid, and labile DOM, such as organic acids, amino acids, aliphatic/proteins, and carbohydrates [36,37]. Studies have shown that both kinds of OM work on reducing Fe and the related As release [38–40]. The simple organic groups are frequently biologically reactive, while refractory DOMs like HA are chemically reactive [32,38,41]. The bioreactive OM enhances the microbial reactivity and provides electrons to reduce the redox potential of groundwater [42,43], thereby promoting the reductive dissolution of Fe oxide minerals [44,45]. The HA is found to work as the electron shuttle to enhance the microbial reduction process, escalating the Fe reduction and As release [46–48]. Moreover, the characteristic of OMs impact the redox conditions of groundwater further, leading to the unpredictable release of redox-sensitive As.

Furthermore, the intensive studies on the natural release of groundwater As from aquifer sediments, and recent studies have highlighted the importance of anthropogenic activities on groundwater As mobilization. The change in groundwater redox conditions is always the reason for this mobilization case. The infiltration of OM, redox-sensitive components, as well as the variation of groundwater table and flow conditions all contribute to the redox condition changes [16,21,49,50]. A study from the Coakley Superfund Site (NH) has shown the microbial decomposition of benzene and other organics from landfill leachate that leads to landfill-stimulated Fe reduction and As release [51]. The *in situ* injection of molasses nitrate shows that organic carbon or its degradation products may quickly mobilize As, and the oxidants may lower As concentrations [11]. Groundwater recharge from ponds carries the degradable organic carbon into the shallow aquifer, and the groundwater flow drawn by irrigation pumping transports pond water to a depth where dissolved As concentrations are greatest [52,53]. With the occurrence of As-bearing Fe–Mn oxides/hydroxides in sediment, the potential of As release mostly depends on the reactivity of OM, which could be sediment oriented, recharged by groundwater, or input of anthropogenic activities. Due to the prevalence of As-bearing Fe–Mn oxides/hydroxides in sediment [20,54], human-oriented OM could be an important stimulus causing groundwater As contamination.

We collected As-bearing sediments from field aquifers for microculture experiments and selected small molecular organic matters that microorganisms could easily use to ensure high microbial reactivity. The experiments were set at a relatively high organic matter concentration with both bioreactive simple organic groups and chemically reactive refractory OM, simulating the maximum limit of As release under anthropogenic activities. Furthermore, it allows for evaluating the risk of As release under extreme conditions of high dose organic carbon penetration, which has significance for the management and control of environmental risks caused by the leakage and infiltration of surface-derived exogenous organic matter (EOM) like landfill leachate and petroleum pollutants.

2. Materials and methods

2.1. Field sample collection and characterization test

The sediment samples were collected in the eastern part of the Jiangnan Plain, belonging to the Quaternary Holocene (Q_4) stratum. The subsurface pressurized water around the sampling site has a closer hydraulic connection with the Yangtze River. It is influenced by the changes in the rise and fall of the Yangtze River water. As (0.75 ± 0.04 – $42.07 \pm 1.01 \mu\text{g L}^{-1}$, avg. $20.25 \mu\text{g L}^{-1}$, $n = 3$) and Mn (0.93 ± 0.13 – $224.45 \pm 2.70 \mu\text{g L}^{-1}$, avg. $84.78 \mu\text{g L}^{-1}$, $n = 3$) were at high concentrations in the background groundwater samples collected. The sediment taken from the high-As aquifer 20 m below the land surface is primarily gray-black fine to silty sand. The sediment at local depths emits a pungent sulfur odor. Therefore, the aquifer sediments in this area were selected for the subsequent experimental study.

The samples were wrapped with plastic film and aluminum foil immediately after collection, sealed and stored away from light, and brought back to the laboratory. To avoid the changes in the morphology of As and Fe in sediments, continuous extraction experiments were carried out with fresh sediment samples. To ensure that the materials used in every system were consistent, the collected sediments were air-dried at room temperature ($25 \text{ }^\circ\text{C}$) and homogenized through 100 mesh screens. Soil organic matter was quantitatively analyzed using the $\text{K}_2\text{Cr}_2\text{O}_7$ heating method, and the content of the organic matter was $26.1 \pm 0.3 \text{ g kg}^{-1}$. The air-dried sediment samples were freeze-dried and ground (200 mesh) for elemental composition analysis. The hand-held portable XRF instrument (SciAps X-50, USA) was used to determine the sediment mineral composition before and after the experiment, as shown in Tables S1 and S5. Tessier sequential extraction [55] was used to determine different As, Fe, and Mn species in the sediment, the details of which are shown in Tables S2 and S3.

2.2. Microcosm setup

Anaerobic microenvironment incubation was repeated in a 100 mL conical flask (containing 7.5 g sediment and 75 mL deoxygenated artificial groundwater) and incubated at $20 \text{ }^\circ\text{C}$ in a N_2 atmosphere in darkness. Sediment samples with higher As content were selected for the microscopic setting. In this study, two different small molecules of DOM (glucose and sodium lactate) and HA representing intractable DOM were tested. All reagents used in the experiment are analytical-grade chemical reagents. The chemical composition of artificial water was similar to that of local groundwater, 0.4 mM CaCl_2 , 0.4 mM K_2SO_4 , and 3 mM NaHCO_3 . The artificial groundwater was sterilized and prepared by autoclaving at $121 \text{ }^\circ\text{C}$ for 25 min [56]. Table 1 revealed the concentration of glucose, sodium lactate, and HA in different experimental groups. Samples were taken regularly at 1, 3, 6, 10, 15, 20, 30, and 60 d time points. At each sampling site, two treatment vials were destructively sampled in the glove box for further geochemical and microbial community analysis.

2.3. Geochemical analysis

Various hydrochemical parameters of each leachate sample were determined, including pH, redox potential (ORP), Fe(II), Fe, Mn, As, anions, and DOC concentrations. pH and ORP were determined immediately after sample collection using an FE-28 standard pH meter (Mettler-Toledo, Greifensee, Switzerland). Fe(II) was tested using a UV–visible spectrophotometer (HACH DR6000,

Table 1
The setting of experimental groups.

Experimental group	Organic matter type and concentration setting	Experimental solution
H	No carbon source addition	Na ⁺ (69 mg L ⁻¹), K ⁺ (8 mg L ⁻¹), Ca ²⁺ (16 mg L ⁻¹), HCO ₃ ⁻ (183 mg L ⁻¹), Cl ⁻ (28 mg L ⁻¹), SO ₄ ²⁻ (10 mg L ⁻¹)
G	Glucose (500 mg L ⁻¹)	
I	Glucose (500 mg L ⁻¹) + Humic acid (250 mg L ⁻¹)	
J	Glucose (500 mg L ⁻¹) + Humic acid (500 mg L ⁻¹)	
K	Sodium lactate (500 mg L ⁻¹)	
L	Sodium lactate (500 mg L ⁻¹) + Humic acid (500 mg L ⁻¹)	

USA). All samples were filtered via a 0.45 µm filter membrane, placed in three 10 mL plastic centrifugal tubes and a 10 mL glass bottle, and stored in the refrigerator at 4 °C. One sample used to test the contents of As, Fe, and Mn was added to 1:1 HNO₃ to make the pH less than 2. One sample was added to a 0.125 M EDTA solution to determine As(III) and As(V), and another was used to test for anions. DOC samples were collected in 10 mL amber bottles and acidified to pH < 2 using H₃PO₄.

An inductively coupled plasma atomic emission spectrometer (ICP-AES, ICAP6300, Thermo) was used to analyze a 10 mL extraction solution to determine the Fe and Mn contents of each sample. The detection limits and precision were 10 µg L⁻¹ and 2%. After filtration, the total As concentration was determined by inductively coupled plasma mass spectrometry (7900 ICP-MS). The detection limit and precision of total As by ICP-MS were 0.01 µg L⁻¹ and 2.8%. The main anions (Cl⁻, SO₄²⁻) were determined via ion chromatography (ICS 2000, Dionex) with an analytical precision of 3%. DOC concentration was measured using a total organic carbon analyzer (TOC-L, Shimadzu, Japan).

The content of As species (primarily As(III) and As(V)) was determined by a high-performance liquid chromatography-hydride generation atomic fluorescence spectrometer (HPLC-HG-AFS). The As(III) and As(V) were separated by chromatographic columns, which included chromatographic columns (11.2 mm, 12–20 µm) and PRP-X100 anion exchange columns (10 µm, 250 × 4.1 mm). The mobile phase was prepared using 20 mM NaH₂PO₄ and 3.5 mM Na₂HPO₄ at a flow rate of 1.0 mL min⁻¹. The retention time of the As species in the sample was compared to that of the standard substance (GBW08666-GBW08667). The concentration was calculated via the peak area. The detection limit and precision were 0.1 µg L⁻¹ and greater than 8%.

The glassware used in the experiment was soaked in 10% HNO₃ for 4 h, rinsed three times with ultra-pure water, and then dried for 4 h at 180 °C. The experimental water used was ultrapure water (Milli-Q, Millipore, ≥18.2 MΩ cm). To ensure data quality, each experiment was conducted using 2–3 analytical tests on samples obtained at each time point. The standard deviation of all analysis methods is within 5%.

2.4. Spectral feature measurement of DOM

Three-dimensional excitation-emission matrix (3D EEM) fluorescence measurement was performed by luminescence spectrometry (F-7000, Hitachi, Japan). The scanning ranges were 200–550 nm for excitation and 280–550 nm for emission. Fluorescence data were collected every 5 nm at the excitation wavelength and every 5 nm at the emission wavelength. The scanning rate was 2400 nm min⁻¹, the slit width was 5 nm, and the voltage amplification was 700 V. To eliminate the Raman scattering peak, each sample subtracts a blank spectrum of ultra-pure water to obtain an average of three spectra, which are recorded under the same conditions.

Three fluorescence indices were calculated: the fluorescence index (FI) is the ratio of emission intensity at 450–500 nm after a

λ_{Ex} 370 nm excitation, providing a metric for differentiating terrestrial and microbial DOM [57,58]. Another index, the biological index (BIX), is calculated from the ratio of the emission intensity of λ_{Em} 380 nm to λ_{Em} 430 nm wavelengths using a fixed excitation of λ_{Ex} 310 nm [59]. Furthermore, the sum of the emission scans at 435–480 nm were divided by the sum of the emission scans at 300–345 nm and at 254 nm excitation to determine the humification index (HIX) [60]. The ratio of UV absorbance to DOC concentration at 254 nm (SUVA₂₅₄) is widely used to reflect the relative content of aromatic structures in DOM [61].

In transmission mode, the functional groups of organic matter in the solution were tested using a Fourier infrared transform spectrometer (Tensor II). It has a spectrum range of 4000 to 400 cm⁻¹ with 16 scanning times and a resolution of 4 cm⁻¹.

2.5. High-throughput sequencing and statistical analysis

The PCR products were amplified and sequenced using the universal 16S rRNA gene primers 338F (5'-ACTCCTACGGGAGG-CAGCAG-3') and 806R (5'-GGACTACHVGGGTWTCTAAT-3') [62,63]. The products were purified via agarose gel electrophoresis and quantified by QuantiFluor™-ST using Pico Green, and the PCR products of equimolar concentration of each sample were collected. The collected products were sequenced on an Illumina Miseq platform at Shanghai Majorbio Bio-pharm Technology Co., Ltd. Operational classification units (OTU) were defined as a unit with a 97% similarity level [64]. On a 97% sequence consistency, the Use arch was used to cluster the most abundant sequences [65]. A Bayesian classifier was used to classify representative sequences [66], and then representative sequences were assigned according to the Silva database [67,68] to obtain the classification information of the bacterial communities. Bacteria are classified according to phylum, class, order, family, and genus.

The relative abundance of different samples can be obtained using the community distribution map of species cladogram, and the relative abundance of different genera in different sample classifications can be compared. Canonical correspondence analysis (CCA)/Redundancy analysis (RDA) was used to explore the relationship among environmental factors, samples, and microbial communities.

CCA/RDA and heatmap plots were obtained by R (version 3.6.2) using vegan and ggplot2 packages. The community distribution map of the species cladogram was made using Graphlan (<https://github.com/biobakery/graphlan>).

3. Results

3.1. Characteristics of microenvironmental changes associated with As release

With the addition of OM, As, Fe, and Mn were significantly released from the sediment. In general, As, Fe, and Mn concentrations increased first and then decreased during the experiment (Fig. 1). The As(III) was the dominant As species as its variation was

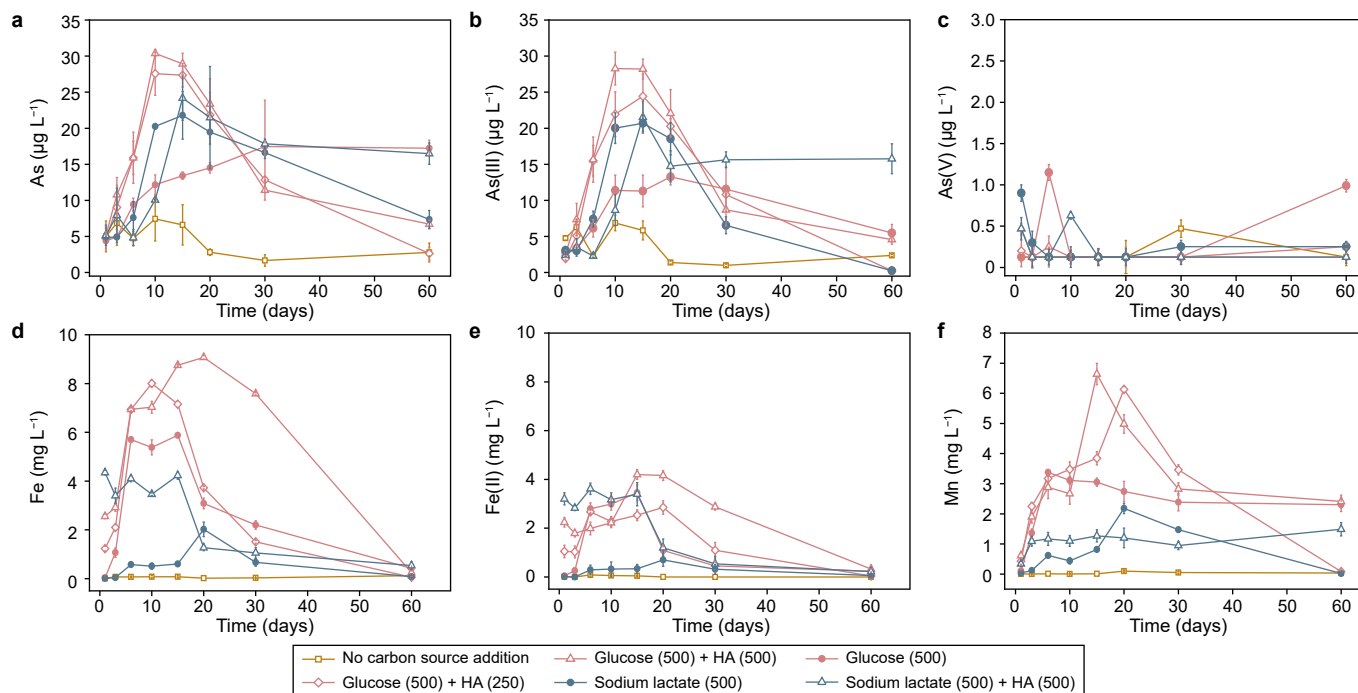


Fig. 1. Variation of As (a), As(III) (b), As(V) (c), Fe (d), Fe(II) (e), and Mn (f) in solution with sediment stimulated by organic matter. Samples with As(V) or As(III) below the detection limit of $0.25 \mu\text{g L}^{-1}$ were plotted as half of the detection limit ($0.125 \mu\text{g L}^{-1}$) to make the comparison. The error bar is the standard deviation ($n = 4$).

consistent with total As (Fig. 1a, b, and S1). The concentration of As(V) was almost lower than the detection limit (Fig. 1c). The trend of Fe(II) was consistent with the total amount of Fe (Fig. 1d and e), and the variation of Mn was similar to Fe (Fig. 1f). In this experiment, As, Fe, and Mn concentrations in each experimental group reached a maximum value in 10–15 days. The results showed significant differences in the biological reduction of Fe(III) and As(V) in experimental groups with different small molecular weight organics and different concentrations of HA. The maximum Fe(II) levels of 0.8 (250 mg L^{-1} HA) and 1.2 times (500 mg L^{-1} HA) and the maximum As(III) levels of 1.8 and 2.1 times were detected in the HA groups compared with the glucose alone group. HA has a more apparent promoting effect on As mobilization, and the effect of high HA concentration on Fe and As mobilization is more significant. Compared with the experimental group with sodium lactate alone, the effect of HA on Fe release was more apparent. The experimental group supplemented with sodium lactate alone showed the same trend of As release compared with the experimental group supplemented with sodium lactate and HA simultaneously; however, the difference in the amount of As release was not significant.

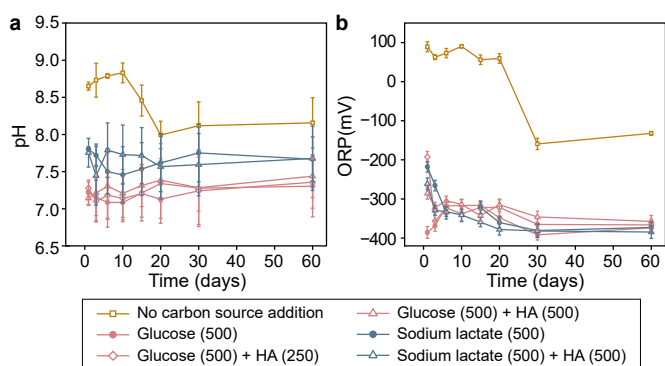


Fig. 2. The change of pH value (a) and ORP (b) with time. The error bar is the standard deviation ($n = 4$).

In Fig. 2a, except for the experimental group without exogenous OM, the pH value of the suspension in other experimental groups remained relatively stable (glucose: 7.0–7.5, sodium lactate: 7.5–8.0). At the beginning of the experiment, the pH value fluctuated in a small range, and at the end, the pH value increased slightly compared with the initial value. It was found that the ORP value of the experimental group without adding OM was positive (50–100 mV) from day 1–20 and negative (–150 to –100 mV) from day 20–30 (Fig. 2b), indicating that the occurrence of transition from an aerobic environment to an anaerobic environment. In the other groups, the ORP values decreased significantly at the beginning of the experiment and gradually remained at negative values around –400 to –300 mV.

The Tessier five-step sequential extraction method was applied to extract different As forms, including exchangeable As (E-As), carbonate As (C-As), Fe/Mn oxide combined As (Fe/Mn-As), organic combined As (O-As), and residual As (Res-As) (Fig. 3a).

The E-As is the As adsorbed in soil, humus, and other components by diffusion and outer complexation. It is sensitive to environmental changes and easy to migrate and transform. The exchangeable state can be extracted from sediment samples by ion exchange. The proportion of E-As in sediment is 1.78%, which is relatively low.

The C-As is the adsorption of As from the sediment onto the carbonate minerals. The C-As is greatly affected by environmental conditions, especially pH. When pH drops, As is easily re-released into the environment. When the pH is increased, it is favorable for carbonate formation. Similar to the exchangeable state, the proportion is 2.89%, and the content is low.

The Fe/Mn oxide binding state is primarily adsorbed or coprecipitated As via the reactive Fe–Mn oxide. The proportion of Fe/Mn-As is larger (3.41%), and the reactivity is higher in anaerobic environments, which readily dissolve As through reductive dissolution.

The O-As are different forms of As wrapped into organic particles and chelated with OM. When organic materials are degraded,

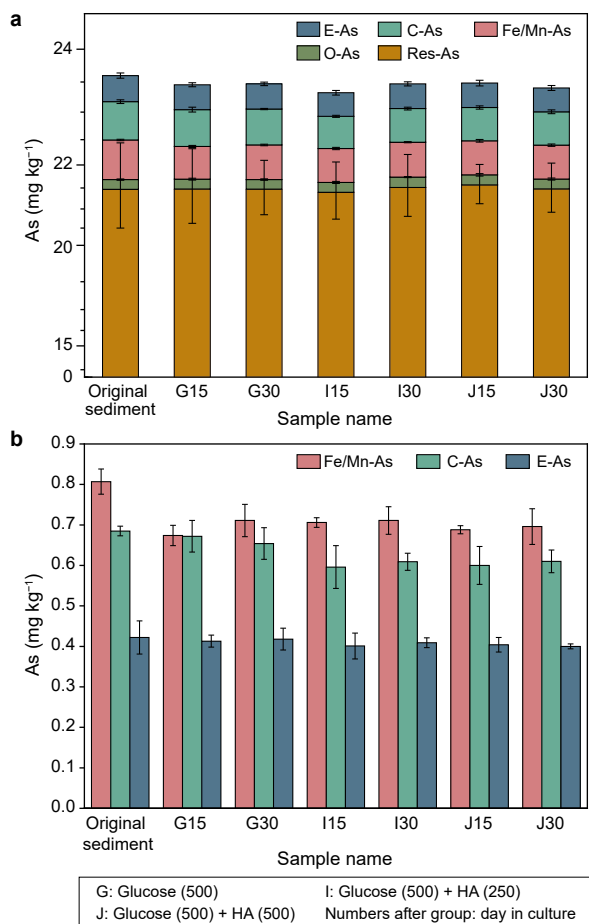


Fig. 3. The variation of different forms of As in sediment. The error bar is the standard deviation ($n = 4$).

soluble trace metals are released, and the proportion of this form is 0.92%.

The main component of Res-As generally exists in the crystal lattice of silicate and primary and secondary minerals and is not easily released under natural conditions. Res-As is stable in the sediment for extended periods with poor bioavailability and accounts for 90.68% of the total content, and the migration is not large; however, the long-term stay when the natural and man-made conditions change may also bring risks.

Compared to the original sediment, the content of E-As (0.9–5.2%), C-As (1.9–13.0%), and Fe/Mn-As (11.9–16.5%) decreased in the sediment after incubation, while the content of O-As (~5%) and Res-As (~0.5%) increased with the concentration of HA. With the increase of HA concentration ($J > I > G$), the decrease of Fe/Mn-As was more significant (Fig. 3b), suggesting that the main source of As release into the solution is Fe/Mn-As. Comparing the changes of different bound As contents in sediments at different time points under the same OM conditions, it was found that the content of Fe/Mn-As decreased significantly, while the content of O-As and Res-As increased.

3.2. Spectral properties of DOM in sediment extracts and aqueous solutions

The HIX <1.5 indicates that DOM mostly originates from biological sources [59]. The experimental groups (H, G, and K) without artificial HA showed strong biogenic characteristics, but the HIX

index of the three groups increased with time. At the end of the culture, the humification degree of the three groups increased by 95.4%, 27.5%, and 24.6%. However, the humification degree of the three groups with artificial HA was significantly weakened (Fig. 4a and b). BIX has a strong negative correlation with HIX and SUVA₂₅₄ and a strong positive correlation with FI (Fig. 4c–e).

Through qualitative analysis of the organic matter groups via infrared spectrum, the evolution rule of organic functional groups in sediments of different experimental groups in time is obtained (Fig. 5). Under different experimental stages, the infrared spectra of sediment samples in the experimental system with different carbon sources are similar; however, there are only differences in the intensity of the absorption peaks. There are seven characteristic absorption peaks in total, and the peaks appear at 3630, 2887, 1431, 1030, 788, 522, and 468 cm⁻¹. Combined with the proportion of functional groups, the DOM fractions were primarily composed of polysaccharides, aliphatic groups, and a small number of proteins and humus substances.

3.3. Community composition of microorganisms stimulated by organic matters

Community composition in the solid phase was analyzed after the culture experiment. The abundance proportion of all samples was selected and displayed in the top 200 OTU. The circular area at the branches represents the taxonomic level. The larger the area, the more such sequences are available. In batch experiments, the community structure of the microorganisms was more sensitive to the response of the type of small molecule OM. The release of As is influenced by the microbial species present in the sample and the relative proportions of all taxa. In this study, microorganisms were divided into eight groups at the phylum level. Proteobacteria and Actinobacteria are the dominant species in group H without the addition of EOM. The abundance of Nitrospirae (2.2%), Chloroflexi (3.6%), and Acidobacteria (5.8%) was higher than that of the experimental group supplemented with EOM, while the abundance of Firmicutes (2.7%) was significantly lower. After the addition of EOM, the abundance of Proteobacteria is the highest, followed by Firmicutes, Actinobacteria, and Bacteroides (Fig. 6).

The statistics of the microbial community were further analyzed at the genus level (Fig. 7). The large increase in OM promoted the occurrence of *Geobacter* but also caused the disappearance of *Sphingomonas*. The abundance of OMs caused a substantial increase in the relative abundance of each group of *Clostridium*.

Bacillus and *Aquabacterium* were the most abundant genera retrieved in the microenvironment with the addition of active small DOM molecules (glucose and sodium lactate), while microorganisms related to *Paenibacillus* and *Burkholderiaceae* were the dominant populations with the addition of HA (Fig. 7).

The addition of glucose positively affected the relative abundance of *Bacillus* (2.48–37.3%) and *Paenibacillus* (10.25–24.91%). *Cloacibacterium* was present as the strain distinguished from the sodium lactate-added group. The addition of sodium lactate alone increased the relative abundance of *Aquabacterium* (36.14%), *Arthrobacter* (3.91–10.57%), *Pseudomonas* (3.19%), and *norank_f_Family_XVIII* (13.42%). The simultaneous addition of sodium lactate and HA significantly increased the relative abundance of *Arthrobacter* (10.15%) and *Brevundimonas* (7.13%).

The higher the Shannon index, the higher the microbial diversity. Compared with group H without the introduction of EOM, the community diversity of all experimental groups with the addition of EOM decreased, indicating that the community within the system had good specificity, and the abundance showed an increasing trend with time (Table S4).

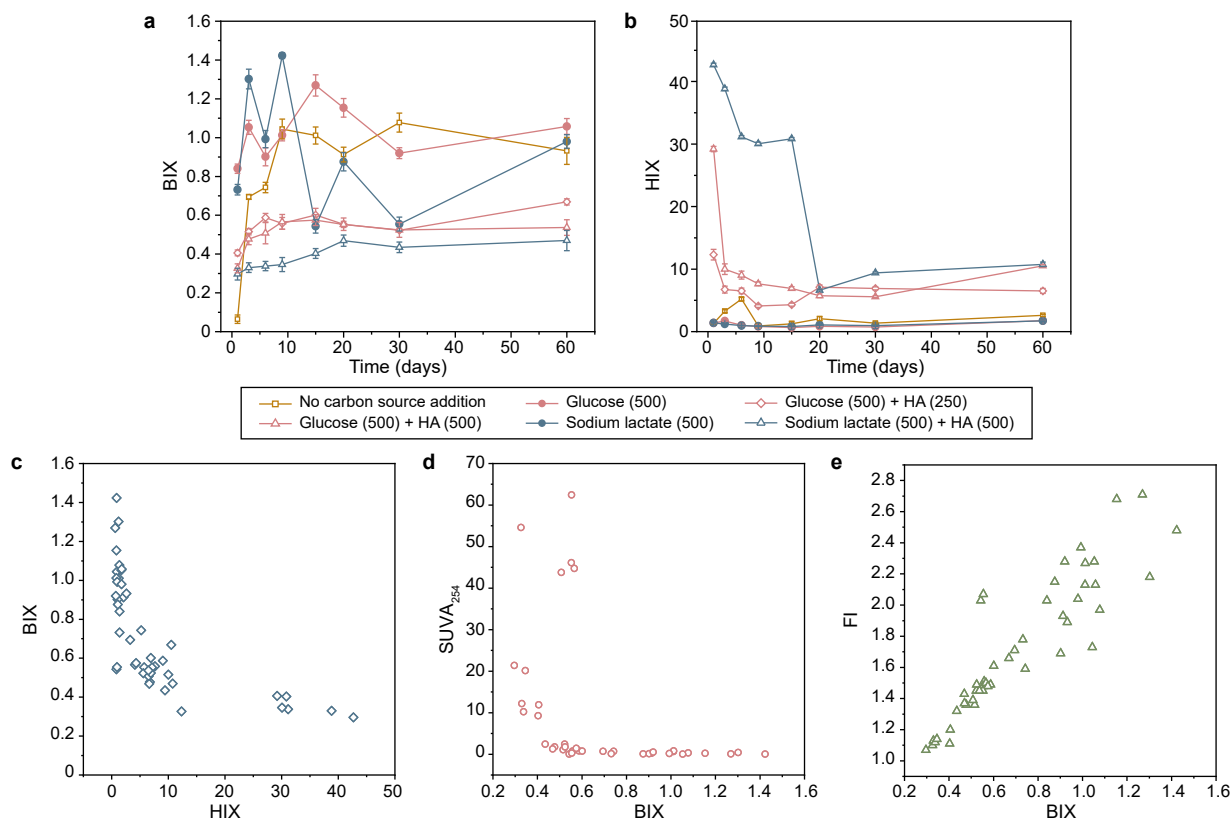


Fig. 4. a–b, The fluorescence index of different experimental groups changed with time: BIX (a) and HIX (b). The error bar is the standard deviation ($n = 4$). c–e, The relationship between HIX and BIX (c), BIX and SUVA₂₅₄ (d), and BIX and FI (e).

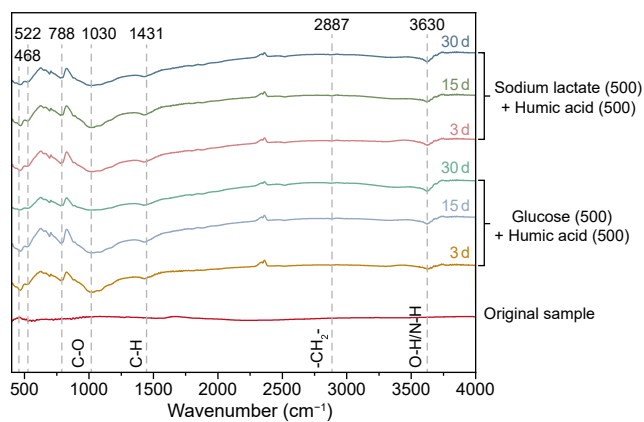


Fig. 5. Band assignment diagram of FTIR spectra of DOM samples extracted from soil.

4. Discussion

4.1. Arsenic release that is contributed by the addition of bioreactive and chemically reactive OM and its influencing factors

Typically, As, Fe, and Mn releases show the same pattern, with a significant increase trend in the first 10–20 days followed by a decline. ORP values indicate reduction conditions that match the dominant reducing species represented by As(III) and an amount of Fe(II) (Figs. 2, S1, and S2). The extraction results of the binding sequence showed a decrease of the Fe/Mn-As form was the largest, which revealed the process of the reducing dissolution of Fe/Mn oxides/hydroxides (Fig. 3). Without the addition of OM, the pure

sediment group shows a very limited release of As ($<5 \mu\text{g L}^{-1}$), Fe ($<0.1 \text{ mg L}^{-1}$), and Mn ($<0.1 \text{ mg L}^{-1}$). In the glucose-supplemented group, the maximum release amounts of As, Fe, and Mn in an aqueous solution was $30.37 \mu\text{g L}^{-1}$, 9.07 mg L^{-1} , and 6.64 mg L^{-1} , respectively, which were higher than those of sodium lactate ($24.17 \mu\text{g L}^{-1}$, 4.35 mg L^{-1} , and 2.18 mg L^{-1}) (Fig. 1). For the microbial community, the use of glucose for energy is easier than sodium lactate and could account for this phenomenon. In the same OM group, As, Fe, and Mn releases are more significant as the amount of HA increases. The release of As, Fe, and Mn under the condition of 500 mg L^{-1} HA was 1.1 times that under the condition of 250 mg L^{-1} HA. The release of As from 500 mg L^{-1} HA was 1.7 times that of glucose alone and 16% higher than that from 250 mg L^{-1} HA. Under 500 mg L^{-1} HA, the release of As, Fe, and Mn was 1.1, 2.1, and 0.68 times that of sodium lactate only. The effect of HA on As, Fe, and Mn release is different from that of bioreactive glucose and sodium lactate, and it is unlikely to be directly utilized by microorganisms. One or more combinations of several processes could contribute to this, including electron shuttling to accelerate electron transfer [69,70], complexation with Fe and As to enhance their aqueous distribution [71], as well as the competitive adsorption with Fe and As absorbed in the sediment [72–74]. Overall this enhanced release achieved by HA is more significant for Fe/Mn than As; the amount of aqueous Fe and Mn could be 1.5 to 3 times more with 500 mg L^{-1} HA than without. However, the elevated concentration of As and Fe is not significant between 500 and 250 mg L^{-1} HA groups (Fig. 1). This indicates that when HA concentration rise to 250 mg L^{-1} , its enhanced effect is almost at a maximum and further increases have limited effect. Other processes could be the limiting factors that regulate the enrichment of As, Fe, and Mn.

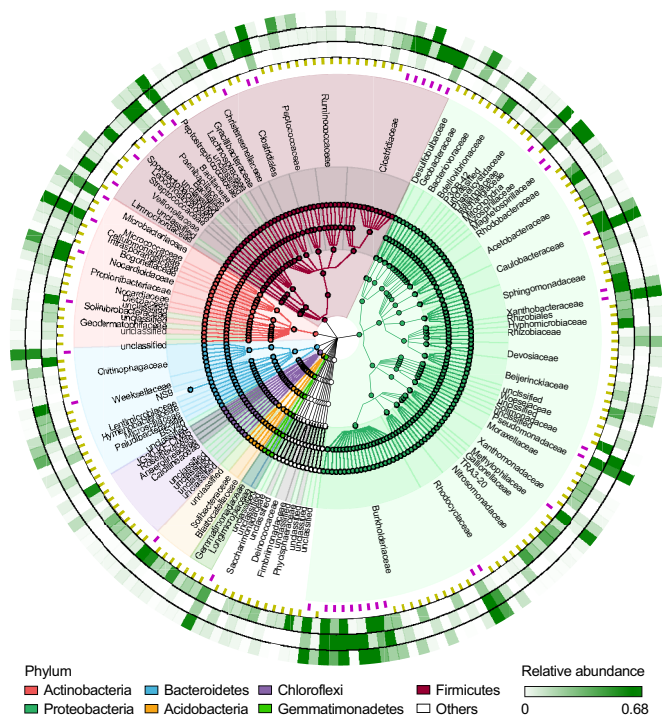


Fig. 6. Community distribution map of species cladogram. In the middle of the graph is the species evolution classification tree. Different colors represent different phyla (refer to the color legend for details). The outer ring shows the thermal circle drawn according to the relative abundance. Each ring represents different sample groups. From the inside to the outside in proper sequence, it represents the sample group with (1) relative abundance greater than 5%, (2) relative abundance less than 5%, (3) group H without OM, (4) groups G, I, and J with glucose, and (5) groups K and L with sodium lactate. The relative abundance is shown in green with different transparencies in different rings, and the darker green with lower transparency represents the higher relative abundance.

The decline of aqueous As, Fe, and Mn could be related to the formation of various secondary Fe minerals, including siderite and mackinawite, which can incorporate As [30,75,76]. This is

evidenced by the changes in the number of key elements in the sediments (Fig. 3; Table S5), which shows that the content of As did not change significantly since its release into aqueous conditions is limited to several dozens of $\mu\text{g L}^{-1}$. However, the amount of sediment Fe was significantly reduced compared with the original ones. In the case of the coexistence of glucose and HA, Fe content in the sediment decreased by 1.4% and 3.1% after 3 and 15 days of incubation, respectively, and increased by 10.9% on day 30. In the presence of sodium lactate and HA, Fe content in the sediment decreased by 8.6% only on day 3 but increased by 0.2% and 9.1% after 15 and 30 days of incubation, respectively. Furthermore, with aqueous Fe, sediment Fe shows its lowest content around 15 days, followed by a slight increase after 30 days. Moreover, the content of S was significantly higher than that of the original sediments, indicating the possible formation of FeS.

4.2. Characteristics of DOM and microbial community indicate microbe-mediated As release

With the decomposition of DOM by the microorganism, the characteristics of DOM could reflect this biological process. The HIX <1.5 indicates that DOM originates from biological sources [59]. The experimental groups (H, G, and K) without artificial HA showed strong biogenic characteristics, while the humification degree of the three groups with artificial HA was significantly weakened (Fig. 4a and b). The results showed that bioreactive glucose, sodium lactate, and chemically reactive HA were all involved in the reaction. In the experimental group supplemented with glucose, the HA concentration of the group with higher concentrations of HA decreased significantly (80.9%), and the HA concentration of the group with a lower concentration of glucose decreased by 66.8%. Compared with the 500 mg L^{-1} HA group, the humic reduction degree of the experimental group supplemented with sodium lactate was slightly higher than that of the group supplemented with glucose, which was 84.5%. The FI index value of 1.4 or lower indicates that DOM comes from a terrigenous source, and a value of 1.9 or higher indicates material of a microbial origin [57]. The SUVA₂₅₄ can be used to illustrate the aromatization of OC and is a good indicator for determining the humic components of OC [77], which is related to the content of aromatic hydrocarbons and

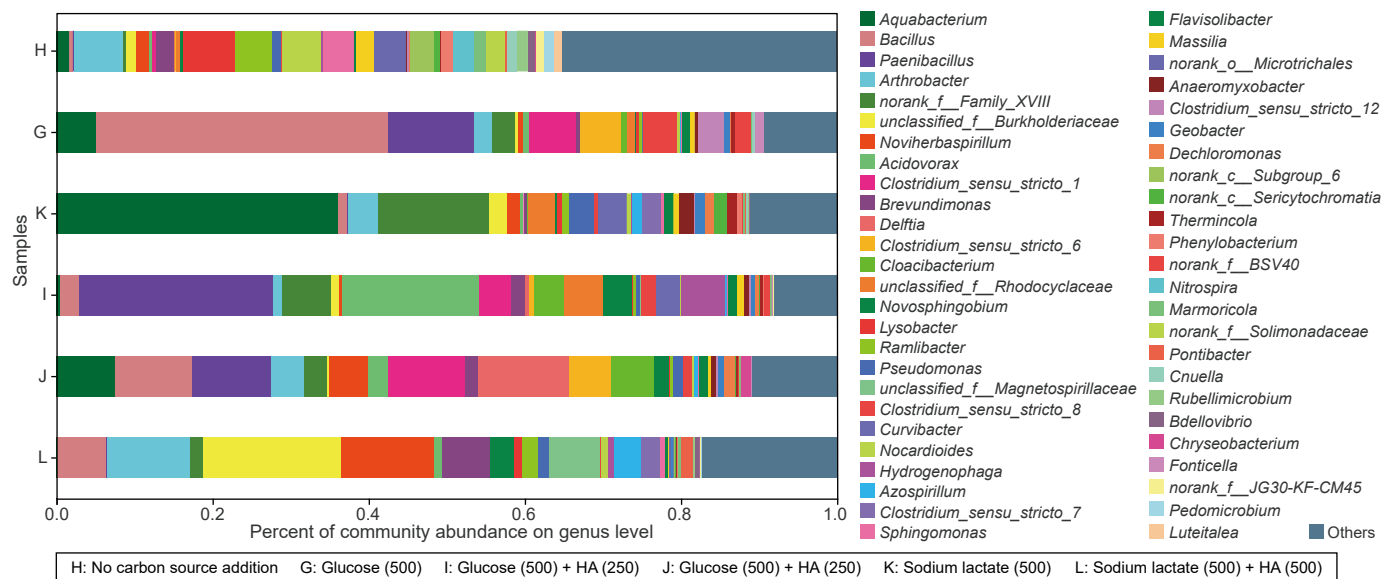


Fig. 7. Histograms of relative abundance of genus community of each experimental group. Those with less than 1% relative abundance were grouped in "Others".

humus-like organic matter macromolecules. BIX has a strong negative correlation with HIX and SUVA₂₅₄ and a strong positive correlation with FI (Fig. 4c–e), meaning that when OM is derived from biological sources, other sources of OM are scarce. Most studies showed that OM, which promotes the mobility of As, was characterized by bioavailability [78–81].

The band at 3750–3000 cm⁻¹ is formed by stretching N–H or O–H bonds of phenols, alcohols, carboxylic acids, and/or other substances containing hydroxyl groups [82]. The proportion of infrared peak areas of the experimental group J decreased gradually during 3–30 days (Fig. 5), indicating that the carboxylic acids and alcohols in the humus were degraded and transformed due to the role of microorganisms in the system. However, the proportion of the infrared peak area of the experimental group L increased first. Then it decreased, indicating that there was not only degradation and transformation of humus but also the release of natural organic matter on day 15. The C–H peaked at approximately 2900 and 1434 cm⁻¹, which are the diagnostic values of amino acids, indicating that the microorganisms produced amino acids through protein-like substances. The peak values of C–O at 1000 cm⁻¹ and C–H at 1400 cm⁻¹ indicate the presence of polysaccharides [83]. In the experimental groups J and L, the C–O functional groups of polysaccharide and polysaccharide were the main functional groups, and their percentage first increased and then decreased. This may be due to the hydrolysis of some polysaccharides to produce a large number of substances with C–O functional groups, and the subsequent decrease in percentage indicates that the microorganisms use polysaccharides for growth and metabolism.

Canonical correspondence analysis (CCA) or redundancy analysis (RDA) was used to investigate the effects of the environmental factors and microbial community distribution and to evaluate their effects on As mobilization. For detrended correspondence analysis (DCA), the size of the first axis is used to determine the choice of RDA or CCA that is greater than or equal to 3.5 to choose a CCA and less than 3.5 to choose an RDA. Through VIF variance expansion factor analysis, the environmental factors with VIF >10 were removed, and the environmental factors with smaller collinearity were reserved for CCA or RDA (Tables S6 and S7). To identify the response relationship between different indexes and As release mediated by microorganisms in the experimental groups supplemented with HA and the experimental groups supplemented with only small molecular organic matter, the former is suitable for an RDA model, and the latter is suitable for a CCA model (Fig. 8a and b). CCA and RDA analysis results showed that As(III), Fe, and Mn were positively correlated with each other and negatively correlated with ORP. The difference was that Fe and BIX were positively correlated in the CCA model adopted by the experimental groups supplemented only with small molecular organic matter, indicating that biological action promoted the dissolution of Fe minerals and the reduction of Fe into the aqueous phase. As, BIX, and HIX had negative correlations, which we observed in the later system, though they still had strong biological activity, the release quantity of As significantly declined. In the RDA model, As(III), Fe, and Mn all showed positive feedback effects from microbial activities but only weakly negative correlation with the added humus, indicating that the higher the humification degree of artificially added humus is not the most controlling factor regulating As mobilization.

Common in the *Actinomycetes* and *Firmicutes* experimental group, there have been reports of high As groundwater sediments [84,85]. *Pseudomonas* [86,87], *Bacillus* [88], *Brevundimonas* [89], *Sphingomonas* [90], and *Flavobacterium* [91] have been identified as bacteria related to As metabolism. These bacteria are also involved in this experiment, indicating that they may play a key role in the As mobilization in the environment.

The relationship between environmental factors and microbial

community was evaluated by using the CCA model, considering the results of all the experimental groups. The amount of interpretation for the first axis of CCA was 14.93%, and that of the second axis was 10.23%. After a significance test, pH ($p = 0.001$), ORP ($p = 0.002$), Mn ($p = 0.041$), and As(III) ($p = 0.002$) were the key influencing factors. The contribution rate of pH, ORP, Mn, TOC, and Fe to the first axis was higher. ORP, Fe, Mn, and As(III) contributed more to the second axis (Table S8). Due to the short length of the arrow representing Fe and TOC, the interpretation of the species lacks universal representativeness.

In the current study, CCA results show that Fe and Mn have strong homology and a significant positive correlation with As(III). *Arthrobacter*, *Burkholderia*, and *Noviherbaspirillum* were primarily affected by environmental factors such as pH and ORP. *Aquabacterium* and *norank_f_Family_XVIII* were affected by As(III). The TOC concentration affected the species of *Paenibacillus*, *Acidovorax*, *Clostridium*, *Delftia*, and *Bacillus*. Group H without organic matter was primarily affected by environmental factors. On days 15 and 30, the samples of each experimental group were closely related to the release of Fe, Mn, and As in the aqueous phase (Fig. 8c).

It has been proven that there is Fe-reducing bacteria in groundwater system, such as *Aquabacterium* sp. and *Clostridium* spp., in sediments of the Hetao Basin [92]. These indigenous Fe-reducing bacteria play a key role in the migration of As within the aquifer. The release of As and the reduction of Fe in the aquifer occur simultaneously [78].

Clostridium can grow in anaerobic environments, ferment organic matter, and reduce metal ions (transition metals), including As. The reduction of Fe(III)/As(V) may not be directly related to electron transport but is indirectly mediated by H₂ produced by *Clostridium* [93]. *Clostridium* can reduce soluble Fe(III) or amorphous Fe(hydr) oxides and combine with DOC oxidation to promote As migration [94]. In addition, studies have shown that under anaerobic conditions, As(V) metabolizing bacteria have been isolated from some sediment belonging to *Bacillus*, which can use lactate or sulfide as electron donors for the biochemical cycling of As [86].

In our experiments, we identified the following bacteria at the genus level with potentially relevant (functioning in aquifer environments) metabolic properties: (1) Fe/Mn/As-reducing bacteria (*Geobacter*, *Pseudomonas*, *Bacillus*, and *Clostridium*), (2) bacteria that can use lactic acid, glucose and other organic carbons for metabolism/fermentation (*Paenibacillus*, *Acidovorax*, and *Delftia*), and (3) degrading bacteria that can use short-chain fatty acids and aromatic compounds as carbon sources (*Sphingomonas*). Previous studies have described these microorganisms to affect As mobilization [88,90]. The relative abundance of some microbial colonies may not be high in the above analysis, but they have a crucial role in controlling As, Fe, and Mn releases. More studies have shown that small and even rare organisms have an active population and can play an important role in biogeochemical processes [95].

4.3. Pollution risk of groundwater As release under EOM

The reactivities of Fe in sediments and organic carbon must be considered in conjunction with the ability of microbiologically driven As and Fe to be released into groundwater by reductive dissolution. Under appropriate hydrogeochemical conditions, especially when OM acts as an electron donor, Fe oxides in aqueous media will undergo reductive dissolution and be released via surface adsorption or bound As [2,79]. During this process, the reactivity of OM is a very important factor. If the organic matter has strong biological reactivity and is easily used by microorganisms, reducing Fe oxides and releasing As are more likely to occur [96]. In Florida, all anaerobic cases show that As was released through

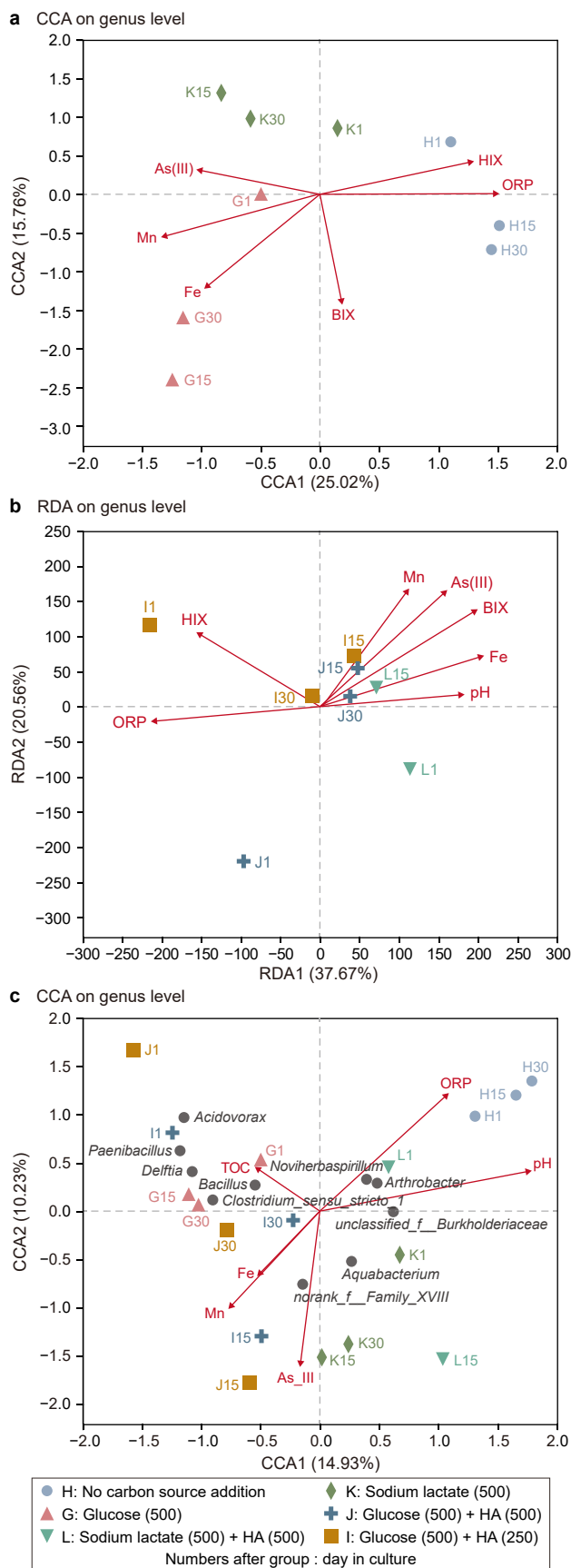


Fig. 8. The correlation between experimental samples and environmental factors in batch experiments. Red arrows in the CCA/RDA diagram represent environmental

reductive dissolution during anaerobic periods. The addition of DOM promotes reductive dissolution, but the addition of refractory DOM (i.e., soil extract) had no effect [97]. In the sediments of the Yangtze River Basin [98], the anaerobic culture resulted in the release of As into the solution, and the terrestrial OM in the sediments had sufficient reactivity to support the microbial reduction of As(V) and Fe(III) in the absence of EOM. In this experiment, the highest concentration of As released in the control group without the addition of EOM was only $7.44 \mu\text{g L}^{-1}$, indicating that the reactivity of terrestrial OM in the sediments was insufficient to support the reduction of As by microorganisms.

Very limited As release ($0.96 \mu\text{g L}^{-1}$) under natural conditions (DOM = 6.9 mg L^{-1}) was observed, while the release of As increased significantly with the addition of glucose [99]. Studies have also shown As < $10 \mu\text{g L}^{-1}$ in groundwater with low DOM, and As release increased with the addition of sodium lactate [100]. The above experimental results indicated that labile OM content might be one of the limiting factors, with EOM significantly stimulating As mobilization even being previously suppressed. In this experiment, the highest concentration of As released after adding extremely high concentrations of small molecule OM was only $21.78 \mu\text{g L}^{-1}$. As release after HA addition increased to $30.37 \mu\text{g L}^{-1}$. However, it was still lower in order of magnitude than the results of some other sediment incubation studies (Table 2). The As concentration measured in 24 groundwater sampling sites were generally in the tens of $\mu\text{g L}^{-1}$ (0.75 ± 0.04 – $42.07 \pm 1.01 \mu\text{g L}^{-1}$, avg. $20.25 \mu\text{g L}^{-1}$, $n = 3$). Analysis of the results of this experiment and the column study with the same sediment (unpublished data) showed that the concentration of As were consistent with the actual situation in the field (Fig. 9).

In the study by Sun et al. [117], it was found that the addition of different OM resulted in different degrees of As release. However, compared with Lawson's study [95], the sediment used by Sun et al. [117] had high As content, and the added OM concentration was much higher than the actual OM concentration in groundwater, while the As concentration did not exceed the detected As concentration in groundwater. It was found that the release of As was only $4.67 \mu\text{g L}^{-1}$ after adding a large amount of OM, which was quite different from the actual As concentration in groundwater [120]. In this case, the effect of EOM on As release is complex and controlled by other factors. The process of releasing As from different sediments cannot be completely reproduced under similar conditions. This inconsistency may also be attributed to different mineral compositions. The reactivity of Fe/Mn oxides may be the reason. Studies show the concentration of As in groundwater does not appear to be dependent on the As content in the solid phase (Table 1). The percentage of Fe/Mn oxide-bound As varied from 48.3% to 98.7% [99], while in the present study, the percentage was 42.2%. The chemical reactivity of different Fe oxide types also varied significantly, with microorganisms preferentially using Fe(III) with low crystallinity, small particle size, high reactivity of hydrous Fe ore, and relatively low reactivity of minerals such as hematite ($\alpha\text{-Fe}_2\text{O}_3$), goethite ($\alpha\text{-FeOOH}$), magnetite ($\gamma\text{-Fe}_3\text{O}_4$), lepidocrocite ($\gamma\text{-FeOOH}$), and hydroxy iron oxide ($\beta\text{-FeOOH}$) [123,124]. High-reactivity goethite or hematite exists in the sediments of the fluvial and lacustrine phases (e.g., Red River Delta and Mekong River Delta), with ferrihydrite and/or lepidocrocite existing in deep layers [44,125–127]. NOM can also drive the release of As and Fe if the sediment minerals primarily comprise Fe hydrates. Therefore,

factors, and the length represents the degree of influence on species. The acute angle between arrows represents a positive correlation, the obtuse angle represents a negative correlation, and the right angle represents no correlation. The projection size of the sample point of the environmental factor arrow indicates the relative influence degree of environmental factors of the sample community distribution.

Table 2
Arsenic release patterns with different characteristics of geogenic and exogenous organic matter

As content		Natural organic matter		Exogenous organic matter	Maximum As release in incubation experiments ($\mu\text{g L}^{-1}$)	Solid-liquid ratio	References
Sediment (mg kg^{-1})	Groundwater ($\mu\text{g L}^{-1}$)	SOM (wt.%)	DOM (mg L^{-1})				
-	1.9–850 217 (avg)	-	High-As: 2.16–14.7 Low-As: 1.7 –5.21 0.8–63.4	-	-	-	[42,96]
Surficial clay deposits: 12 Deeper aquifer sands: 2	2–1100 209 (avg)	-	-	-	-	-	[95]
-	215–224	SYII9: 0.64 SYII28: 0.07	-	50 mM acetate 50 mM acetate + 50 μM AQDS	SYII9: 400 $\mu\text{g g}^{-1}$ SYII28: 46 \pm 2 $\mu\text{g g}^{-1}$	1:2	[56]
-	76–1093	-	2.31–12.88	-	-	-	[101]
-	S1, S2, S7: b.d.–141 S3, S4: b.d.–342 S6: 9–987	S1: 0.08–0.61 S2: 0.01–0.61 S3–S7: 0.01–0.66	-	-	-	-	[102]
1.5–51.4 m: 0 –107.5 18–20 m: >100 12.7 (avg)	b.d.–1205	18–20 m: 0.04–0.26 1.5–51.4 m: 0.04–2.71 1.03 (avg)	-	2 mM glucose	18–20 m: 24.4 $\mu\text{g g}^{-1}$ Other depths: <1 $\mu\text{g g}^{-1}$	1:5	[49]
-	A: >100 B: <10 92.4 (avg)	-	A: ~10 B: <2	-	-	-	[103]
-	10 m: 7–41 25 m: 47–206	0.14	10 m: about 0–25 25 m: about 0–15	-	-	-	[50]
3.17 \pm 0.81	0.66–2.07 μM	0.07 (avg)	0.39–0.62 mM	30 L sucrose	About 0.5–3 μM	-	[104]
5.0–39.6; Fine-grained: 11.1–39.6; Coarse-grained: 5.0–32.0	3.3–161	Fine-grained: 0.89–2.51; coarse-grained: 0.01–2.01	1.2–35.8	-	-	-	[105]
5.09–12.3 8.03 \pm 2.79 (avg)	20–29800 (mud fluid)	1.15–2.21	141–530	-	-	-	[106]
5.7–26.8 13.45 (avg)	25–1800	b.d.–1.6 (n-alkanes: 1.65–30.44 mg kg^{-1})	-	-	-	-	[107]
LD: 1.2–50.4 TM: 0.5–15.4	LD-HUA: b.d.–42 LD-HPA: 131–314 TM-HUA: 2.3–36 TM-PCA: 25–94	-	LD-HUA: b.d.–8.3 LD-HPA: 15 –53 TM-HUA: 0.3–8.4 TM-PCA: 1.3 –5.5	-	-	-	[108]
-	Wells within geomorphic features: 253 \pm 5.4 Wells in undisturbed flood plain: 47 \pm 1.4	Core I: < 1.5 Core II: < 3	-	-	-	-	[109]
0.08–12.77	30–750 410 (avg)	F: 0.021–0.325 L: 0.023–0.086	0.20–5.09	0.9 g glucose and polypepton	16.77	1:15	[110]
8.5 \pm 0.43 (avg)	500	0.26–0.7	-	-	-	-	[111]
Shallow clay: 21 Deep sand: 40	>1200	Shallow clay: 0.70 Deep sand: 0.16	-	2 mM glucose	-	1:40	[98]

					AOA: 1.07–5.27 to <0.1–6.15 μM (deep) OAO: 0.04–0.35 to <0.25 μM (shallow); 0.3–4.5 to <0.25 μM (deep)			
1.71–15.33 NP1: 3.15 NP3: 8.28 NP8: 3.91	50–440 0.96	4.43–13.67 NP1: 0.09 NP3: 0.12 NP8: 0.31	- 6.9	- 2000 mg C per L glucose	- Without glucose addition: $74.6 \pm 3.9 \mu\text{g kg}^{-1}$ NP1: $138 \pm 32.0 \mu\text{g kg}^{-1}$ NP3: increase (no data) NP8: $11.2 \pm 3.8 \mu\text{g kg}^{-1}$	- 1:4	[112] [99]	
11.7	-	-	-	30 g sodium citrate 30 g glucose	57.2 38.5	1:13.3	[113]	
- As(III): 0.06 ± 0.02 As(V): 7.06 ± 0.95	10–300 <1.0–562.7	b.d.–0.02 0.05 ± 0.02	- -	10 mM sodium acetate 50 mM acetate	6–18 42.9 ± 4.7	1:2 1:2	[114] [115]	
3.1–13.5 PW: 20.9 DW: 16.8	<10 PW: 161–347 DW: 17.1–22.1	- PS: 3.7 DS: 5.8	b.d. PW: 4.41 -8.52 DW: 1.06 -2.90	20 mM sodium lactate 12 mg L ⁻¹ water-extractable organic matter 15 mg L per water-extractable organic matter	45 PW: 452 DW: 159	- 1:5	[100] [32]	
32.4 ± 1.2	112	0.011 ± 0.0012	-	500 μM lactate , 750 μM each of pentadecane and hexadecane , and 500 μM benzoate	403.2	1:4	[116]	
27.06	-	0.156	-	Glucose (0.10, 0.25, 0.50, 1.0, 1.5, and 2.0 g L ⁻¹) Humic acid (same as above) Fulvic acid (same as above)	Glucose (2.0 g L ⁻¹): 348 Humic acid (1.5 g L ⁻¹): about 120 Fulvic acid (2.0 g L ⁻¹): about 280	1:10	[117]	
2.55 24.9	2.0 -	0.0003 -	- -	200, 2000, 20000 mg C per L glucose 9 g acetate 9 g lactate 9 g glucose	Acetate: 511.2 Lactate: about 150 Glucose: about 350	1:1 1:33.3	[118] [119]	
13.4	1500	-	-	70 g C per L glucose 70 g C per L sodium acetate	Glucose: 4.67 Sodium acetate: 7.55	1:16.7	[120]	
7.2 15.8	-	-	-	0.8 g glucose 0.6, 0.9, 1.2 g glucose	50 41, 57, 67	1:16 1:15	[121]	
- <3	>40 640	- -	- -	4 g L ⁻¹ acetate 1.5 mM DOC (lactate)	180 (As(III)) 100	1:2 1:2	[78] [132]	
425.82 ± 40.25	-	0.79 ± 0.04 (TC)	-	5.13 g L ⁻¹ sodium acetate (1.5 g L ⁻¹ TOC) 4.00 g L ⁻¹ sodium propionate (1.5 g L ⁻¹ TOC) 3.44 g L ⁻¹ sodium butyrate (1.5 g L ⁻¹ TOC) 4.67 g L ⁻¹ sodium lactate (1.5 g L ⁻¹ TOC) 3.75 g L ⁻¹ glucose (1.5 g L ⁻¹ TOC)	2198 2648 2606 2357 2446	1:1.2	[122]	
23.601	1.22–1320 93.28 (avg)	0.0306–4.49	-	H: No carbon source addition G: Glucose (500 mg L ⁻¹) I: Glucose (500 mg L ⁻¹) + Humic acid (250 mg L ⁻¹) J: Glucose (500 mg L ⁻¹) + Humic acid (500 mg L ⁻¹) K: Sodium lactate (500 mg L ⁻¹) L: Sodium lactate (500 mg L ⁻¹) + Humic acid (500 mg L ⁻¹)	H: 7.43 G: 17.48 I: 27.57 J: 30.37 K: 21.78 L: 24.17	1:10	This study	

Abbreviations: SOM: soil organic matter; DOM: dissolved organic matter; b.d.: below detection limit; HUA: Holocene unconfined aquifer; PCA: Pleistocene confined aquifer; HPA: Holocene Pleistocene aquitard; F: fine particle fraction of sediments; L: large particle fraction of sediments; AOA: Anoxic-Oxic-Anoxic; OAO: Oxic-Anoxic-Oxic.

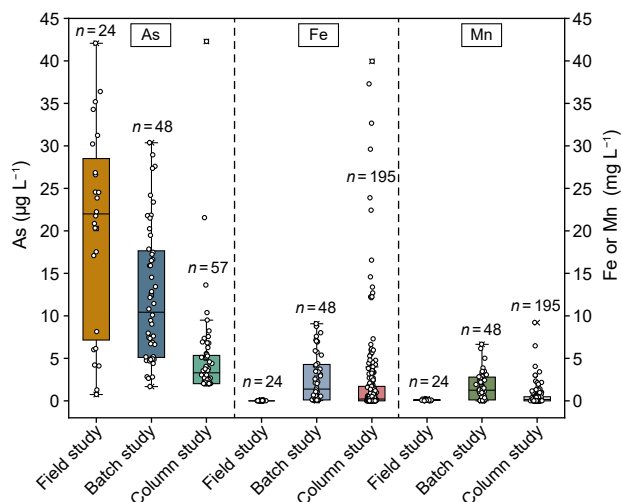


Fig. 9. Comparison of As, Fe, and Mn concentrations monitored in field, batch, and column (unpublished) experiments.

under the same EOM conditions, they have a greater capacity to release As and are more likely to result in higher groundwater As concentrations.

The sediments selected in this study were taken from the high-As aquifer in the Jiangnan Plain, with the measured percentage of Fe content being 9.46%. Previous studies have shown that most of the Fe in the sediments of this region is associated with silicates and contains small amounts of ferrihydrite and hematite and some arsenopyrite within the deeper layers [128]. Based on the order of microbial reduction of Fe(III) from easy to difficult: ferrihydrite > lepidocrocite > hematite [129,130], the extent of As release in this study may be limited by the reactivity of Fe/Mn oxides.

The analysis of the results of the batch experiment and the study of the same sediment column (unpublished data) showed that the concentration of As was consistent with the actual field situation (Fig. 9). The results shown in the batch experiment are cumulative results during the experimental period. The As mobilization/

immobilization equilibrium may be reached during the experimental period. Column studies are more reflective of hydro-geochemical kinetics than batch studies. Precipitation/dissolution reactions may lead to reduced infiltration rates either through clogging (precipitation) or through the dissolution of soil colloids. The water then carries away the dissolved As, promoting the dissolution of the mineral until the reactive mineral source is exhausted. Despite these differences, As was present at concentrations of the same order of magnitude in both batch and column experiments. Under the condition of sufficient active OM, the slow flow rate may result in the enrichment of As and Mn. The range of As concentration detected in groundwater at the actual site was consistent with the simulated results of this experiment. However, the actual site will have a longer flow path, slower flow rate, and more complex water chemical conditions than in our experiment; therefore, the pattern of As distribution and enrichment process may be more complicated.

Although our experiments were microcosm based and did not directly simulate hydrogeological parameters and OM fluxes *in situ*, our results support the theory that high concentrations of EOM contribute to the increased release of sensitive components such as As and Mn. This is supported by the strong biological activity with the addition of EOM. However, the release degree of As and Mn was regulated by the characteristics of EOM and Fe/Mn oxides. Furthermore, its concentration is, to some extent, suppressed by secondary Fe precipitation. We proposed a potential risk of groundwater As migration and transformation affected by EOM infiltration (Fig. 10). In summary, EOM causes the risk of As release, but the risk will not increase indefinitely.

5. Environmental implications

Co-deposition of As-bearing Fe oxide minerals with reactive OMs in the delta/floodplain or river-lake plain sediments is a prerequisite for As release in reductive geochemical settings. OM reactivity is frequently considered a limiting factor for As release in geogenic As-affected areas, such as the Datong Basin (magnetite and hematite) [131], the Hetao Basin (poorly crystalline Fe oxides) [31,101], the Red River, Ganges-Yarlung Tsangpo River, and the

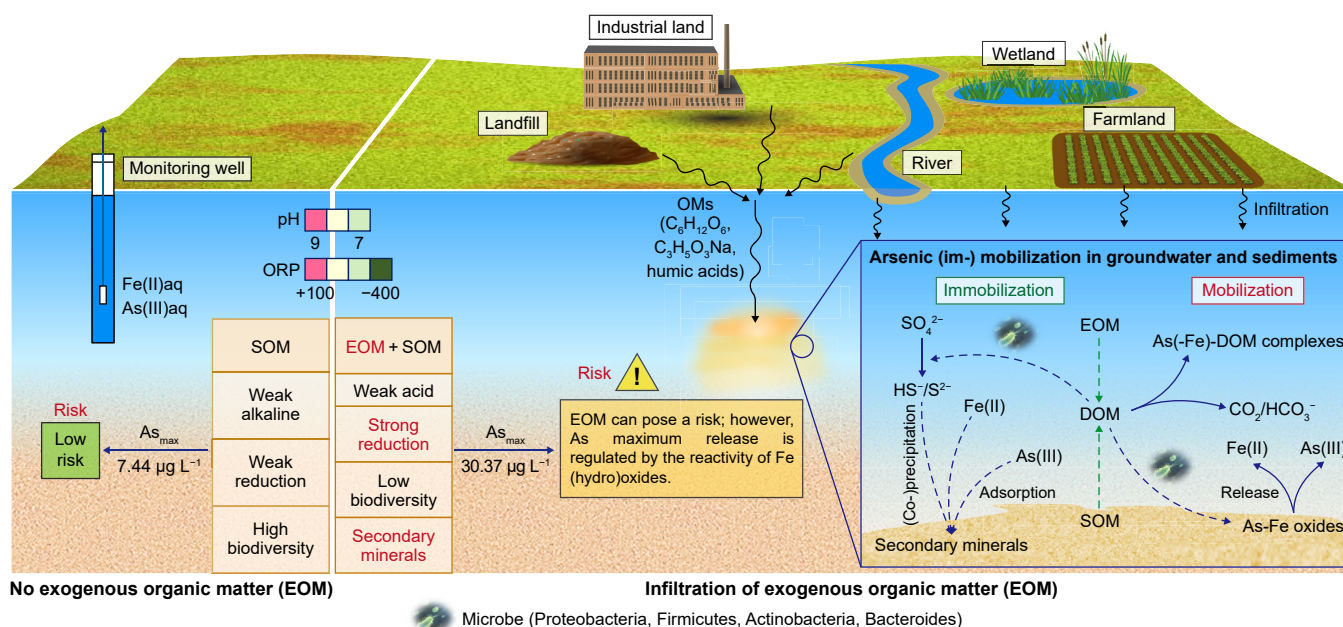


Fig. 10. Conceptual model of groundwater As mobilization with the infiltration of surface-derived EOM.

Mekong River delta in Vietnam. With widespread As-bearing sediment in the shallow aquifers, the input of EOM could be harmful and may trigger the secondary risk of contamination. So in specific sites such as landfills, petrochemical sites, and managed aquifer recharge projects, attention should be paid not only to groundwater contamination caused by direct contaminant input but also the risk of harmful elements like As and Mn release from aquifers triggered by enhanced reducing conditions caused by EOM [3,30].

6. Conclusion

The EOM infiltration enhances As and Mn releases in aqueous solutions, causing the risk of groundwater pollution. The potential release capacity of As from sediment was evaluated under high levels of EOM with both bioreactive and chemically reactive OMs. The OMs were characterized by FI, HIX, BIX, and SUVA₂₅₄ fluorescence indices showing the biological activities were kept at a high level during the experimental period. The infrared spectra of different bands also show the metabolism of polysaccharides and other protein substances and the degradation and transformation of macromolecular humus. Under the stimulation of EOM, Proteobacteria, Firmicutes, Actinobacteria, and Bacteroidetes became the dominant phylum. At the genus level, bacteria that reduce Fe/Mn/As (*Geobacter*, *Pseudomonas*, *Bacillus*, and *Clostridium*) and bacteria that can participate during metabolic transformation using EOM (*Paenibacillus*, *Acidovorax*, *Delftia*, and *Sphingomonas*) were identified.

At very high concentrations of organic matter, the reduction environment promoted As, Fe, and Mn releases. The infiltration of high levels of bioreactive/chemically reactive EOM may participate in As release during microbial dissimilation reduction as a carbon source or an electron shuttle. Moreover, the reactivity and content of EOM are the main external factors for As and Mn enrichment. However, the release of As only increased during the first 15–20 days, followed by a decline, contributed by secondary iron precipitation. The experimental monitoring values were consistent with the *in situ* groundwater monitoring values.

Whether or not EOM infiltration causes a risk to groundwater and its extent depends not solely on the reactivity and concentration of OM but also, as our experiment suggested, on the nature of the reactivity of Fe (hydro)oxides. As the main source of As in groundwater, the reactivity of Fe minerals and the precipitation of secondary minerals are the essential internal factors determining the upper limit of geogenic As releases. However, all these processes are more complex in practical applications, including the effects of hydrodynamics and hydrogeochemical environments, which are worthy of further study.

CRedit authorship contribution statement

Fan Feng: Conceptualization, Methodology, Investigation, Formal analysis, Writing - Original Draft. **Yongfeng Jia:** Methodology, Resources, Writing - Review & Editing, Funding acquisition. **Yonghai Jiang:** Writing - Review & Editing, Supervision, Project administration. **Xinying Lian:** Investigation. **Changjian Shang:** Investigation. **Meng Zhao:** Formal analysis, Validation.

Declaration of competing interest

The authors declare that they have no known competing financial interests or personal relationships that could have appeared to influence the work reported in this paper.

Acknowledgments

The research work was financially supported by the National Key Research and Development Program (2019YFC1806204) and the National Natural Science Foundation of China (No. 41907178).

Appendix A. Supplementary data

Supplementary data to this article can be found online at <https://doi.org/10.1016/j.ese.2023.100243>.

References

- [1] Y. Wang, K. Pi, S. Fendorf, et al., Sedimentogenesis and hydrobiogeochemistry of high arsenic Late Pleistocene-Holocene aquifer systems, *Earth Sci. Rev.* 189 (2017) 79–98.
- [2] M. Glodowska, E. Stopelli, T. Pham, et al., Arsenic behavior in groundwater in Hanoi (Vietnam) influenced by a complex biogeochemical network of iron, methane, and sulfur cycling, *J. Hazard Mater.* 407 (2021), 124398.
- [3] Y.F. Jia, Geogenic contaminated groundwater in China, in: *Global Groundwater Source, Scarcity, Sustainability, Security, and Solutions*, Elsevier, 2021, pp. 229–242.
- [4] A. van Geen, T. Protus, Z. Cheng, et al., Testing groundwater for arsenic in Bangladesh before installing a well, *Environ. Sci. Technol.* 38 (2004) 6783–6789.
- [5] H. Guo, Y. Zhang, L. Xing, et al., Spatial variation in arsenic and fluoride concentrations of shallow groundwater from the town of Shahai in the Hetao basin, Inner Mongolia, *Appl. Geochem.* 27 (11) (2012) 2187–2196.
- [6] L.A. Richards, D. Mangone, C. Sovann, et al., High resolution profile of inorganic aqueous geochemistry and key redox zones in an arsenic bearing aquifer in Cambodia, *Sci. Total Environ.* 590–591 (2017) 540–553.
- [7] D. Polya, C. Sparrenbom, S. Datta, et al., Groundwater arsenic biogeochemistry – key questions and use of tracers to understand arsenic-prone groundwater systems, *Geosci. Front.* 10 (2019) 1635–1641.
- [8] M.M. Shen, H.M. Guo, Y.F. Jia, et al., Partitioning and reactivity of iron oxide minerals in aquifer sediments hosting high arsenic groundwater from the Hetao basin, P. R. China, *Appl. Geochem.* 89 (2018) 190–201.
- [9] J. MCARTHUR, Natural organic matter in sedimentary basins and its relation to arsenic in anoxic ground water: the example of West Bengal and its worldwide implications, *Appl. Geochem.* 19 (8) (2004) 1255–1293.
- [10] R.B. Neumann, K.N. Ashfaq, A.B.M. Badruzzaman, et al., Anthropogenic influences on groundwater arsenic concentrations in Bangladesh, *Nat. Geosci.* 3 (1) (2009) 46–52.
- [11] C.F. Harvey, C.H. Swartz, B. Badruzzaman, et al., Arsenic mobility and groundwater extraction in Bangladesh, *Science* 298 (5598) (2002) 1602–1606.
- [12] C.F. Harvey, K.N. Ashfaq, W. Yu, et al., Groundwater dynamics and arsenic contamination in Bangladesh, *Chem. Geol.* 228 (1–3) (2006) 112–136.
- [13] A. Piepenbrock, S. Behrens, A. Kappler, Comparison of humic substance- and Fe(III)-Reducing microbial communities in anoxic aquifers, *Geomicrobiology* 31 (10) (2014) 917–928.
- [14] P. Li, B. Li, G. Webster, et al., Abundance and diversity of sulfate-reducing bacteria in high arsenic shallow aquifers, *Geomicrobiology* 31 (9) (2014) 802–812.
- [15] T.N. Weng, C.W. Liu, Y.H. Kao, et al., Isotopic evidence of nitrogen sources and nitrogen transformation in arsenic-contaminated groundwater, *Sci. Total Environ.* 578 (Feb.1) (2016) 167–185.
- [16] T.L. Zheng, Y.M. Deng, Y.X. Wang, et al., Microbial sulfate reduction facilitates seasonal variation of arsenic concentration in groundwater of Jiangnan Plain, Central China – Science Direct, *Sci. Total Environ.* 735 (2020), 139327.
- [17] Y.F. Jia, H.M. Guo, Y.X. Jiang, et al., Hydrogeochemical zonation and its implication for arsenic mobilization in deep groundwaters near the Langshan mountains of the Hetao Basin, Inner Mongolia, *J. Hydrol.* 518 (2014) 410–420.
- [18] Y.F. Jia, H.M. Guo, B.D. Xi, et al., Sources of groundwater salinity and potential impact on arsenic mobility in the western Hetao Basin, Inner Mongolia, *Sci. Total Environ.* 601 (2017) 691–702.
- [19] H.M. Guo, Y.Z. Zhou, Y.F. Jia, et al., Sulfur cycling-related biogeochemical processes of arsenic mobilization in the western Hetao Basin, China: evidence from multiple isotope approaches, *Environ. Sci. Technol.* 50 (2016) 12650–12659.
- [20] P. Li, Y. Wang, X. Dai, et al., Microbial community in high arsenic shallow groundwater aquifers in Hetao Basin of inner Mongolia, China, *PLoS One* 10 (5) (2015).
- [21] A.-R. Schittich, U.J. Wunsch, H.V. Kulkarni, et al., Investigating fluorescent organic-matter composition as a key predictor for arsenic mobility in groundwater aquifers, *Environ. Sci. Technol.* 52 (2018) 13027–13036.
- [22] Z.P. Gao, Y.F. Jia, H.M. Guo, et al., Quantifying geochemical processes of arsenic mobility in groundwater from an inland basin using a reactive transport model, *Water Resour. Res.* 56 (2) (2020).
- [23] X.H. Wu, B. Bowers, D. Kim, et al., Dissolved organic matter affects arsenic

- mobility and iron(III) (hydr)oxide formation: implications for managed aquifer recharge, *Environ. Sci. Technol.* 53 (24) (2019) 14357–14367.
- [24] X.L. Cai, L.K. Thomas-Arrigo, X. Fang, et al., Impact of organic matter on microbially-mediated reduction and mobilization of arsenic and iron in Arsenic(V)-bearing ferrihydrite, *Environ. Sci. Technol.* 55 (2021) 1319–1328.
- [25] J.P.M. Vink, A. van Zomeren, J.J. Dijkstra, et al., When soils become sediments: large-scale storage of soils in sandpits and lakes and the impact of reduction kinetics on heavy metals and arsenic release to groundwater, *Environ. Pollut.* 227 (2017) 146–156.
- [26] A.A.D.S. Machado, K. Spencer, W. Kloas, et al., Metal fate and effects in estuaries: a review and conceptual model for better understanding of toxicity, *Sci. Total Environ.* 541 (2016) 268–281.
- [27] Y.H. Wang, G.L. Zhang, H.L. Wang, et al., Effects of different dissolved organic matter on microbial communities and arsenic mobilization in aquifers, *J. Hazard Mater.* 411 (2021), 125146.
- [28] A. Aftabtalab, J. Rinklebe, S.M. Shaheen, et al., Review on the interactions of arsenic, iron (oxy)(hydr)oxides, and dissolved organic matter in soils, sediments, and groundwater in a ternary system, *Chemosphere* 286 (2022), 131790.
- [29] Y.P. Bao, N.S. Bolan, J.H. Lai, et al., Interactions between organic matter and Fe (hydr) oxides and their influences on immobilization and remobilization of metal(loid)s: a review, *Crit. Rev. Environ. Sci. Technol.* (2021) 1–22.
- [30] Y. Jia, B. Xi, Y. Jiang, et al., Distribution, formation and human-induced evolution of geogenic contaminated groundwater in China: a review, *Sci. Total Environ.* 643 (2018) 967–993.
- [31] H. Guo, X. Tang, S. Yang, et al., Effect of indigenous bacteria on geochemical behavior of arsenic in aquifer sediments from the Hetao Basin, Inner Mongolia: evidence from sediment incubations, *Appl. Geochem.* 23 (12) (2008) 3267–3277.
- [32] H. Guo, X. Li, W. Xiu, et al., Controls of organic matter bioreactivity on arsenic mobility in shallow aquifers of the Hetao Basin, P.R. China, *J. Hydrol.* 571 (2019) 448–459.
- [33] W. Xiu, J. Lloyd, H. Guo, et al., Linking microbial community composition to hydrogeochemistry in the western Hetao basin: potential importance of ammonium as an electron donor during arsenic mobilization, *Environ. Int.* 136 (2020), 105489.
- [34] Y. Zhu, Y. Zhai, Y. Teng, et al., Water supply safety of riverbank filtration wells under the impact of surface water–groundwater interaction: evidence from long-term field pumping tests, *Sci. Total Environ.* 711 (2020), 135141.
- [35] Z. Chen, Y.P. Wang, D. Xia, et al., Enhanced bioreduction of iron and arsenic in sediment by biochar amendment influencing microbial community composition and dissolved organic matter content and composition, *J. Hazard Mater.* 311 (2016) 20–29.
- [36] K. Kalbitz, J. Schmerwitz, D. Schwesig, et al., Biodegradation of soil-derived dissolved organic matter as related to its properties, *Geoderma* 113 (2003) 273–291.
- [37] M. Lawson, D.A. Polya, A.J. Boyce, et al., Tracing organic matter composition and distribution and its role on arsenic release in shallow Cambodian groundwaters, *Geochem. Cosmochim. Acta* 178 (2016) 160–177.
- [38] X. Li, H. Guo, H. Zheng, et al., Roles of different molecular weights of dissolved organic matter in arsenic enrichment in groundwater: evidences from ultrafiltration and EEM-PARAFAC, *Appl. Geochem.* 104 (2019) 124–134.
- [39] P. Sharma, J. Ofner, A. Kappler, Formation of binary and ternary colloids and dissolved complexes of organic matter, Fe and As, *Environ. Sci. Technol.* 44 (2010) 4479–4485.
- [40] G. Liu, A. Fernandez, Y. Cai, Complexation of arsenite with humic acid in the presence of ferric iron, *Environ. Sci. Technol.* 45 (2011) 3210–3216.
- [41] R.G. Keil, D.L. Kirchman, Dissolved combined amino acids: chemical form and utilization by marine bacteria, *Limnol. Oceanogr.* 38 (1993) 1256–1270.
- [42] W. Qiao, H.M. Guo, C. He, et al., Molecular evidence of arsenic mobility linked to biodegradable organic matter, *Environ. Sci. Technol.* 54 (2020a) 7280–7290.
- [43] L. Yan, X.J. Xie, Y.X. Wang, et al., Organic-matter composition and microbial communities as key indicators for arsenic mobility in groundwater aquifers: evidence from PLFA and 3D fluorescence, *J. Hydrol.* 591 (2020), 125308.
- [44] J.W. Stuckey, M.V. Schaefer, B.D. Kocar, et al., Arsenic release metabolically limited to permanently water-saturated soil in Mekong Delta, *Nat. Geosci.* 9 (1) (2016) 70–76.
- [45] Z. Zhang, H. Guo, S. Liu, et al., Mechanisms of groundwater arsenic variations induced by extraction in the western Hetao Basin, Inner Mongolia, China, *J. Hydrol.* 583 (2020), 124599.
- [46] N. Mladenov, Y. Zheng, M.P. Miller, et al., Dissolved organic matter sources and consequences for iron and arsenic mobilization in Bangladesh aquifers, *Environ. Sci. Technol.* 44 (1) (2010) 123–128.
- [47] H. Kulkarni, N. Mladenov, K.H. Johannesson, et al., Contrasting dissolved organic matter quality in groundwater in Holocene and Pleistocene aquifers and implications for influencing arsenic mobility, *Appl. Geochem.* 77 (2017) 194–205.
- [48] H.V. Kulkarni, N. Mladenov, D.M. McKnight, et al., Dissolved fulvic acids from a high arsenic aquifer shuttle electrons to enhance microbial iron reduction, *Sci. Total Environ.* 615 (2018) 1390–1395.
- [49] Michael V. Schaefer, Xinxin Guo, Yiqun Gan, et al., Redox controls on arsenic enrichment and release from aquifer sediments in central Yangtze River Basin, *Geochem. Cosmochim. Acta* 204 (2017) 104–119.
- [50] K. Yu, Y. Gan, A. Zhou, et al., Organic carbon sources and controlling processes on aquifer arsenic cycling in the Jiangnan Plain, central China, *Chemosphere* 208 (2018) 773–781.
- [51] J.L. Delemos, B.C. Bostick, C.E. Renshaw, Landfill-stimulated iron reduction and arsenic release at the Coakley superfund site(NH), *Environ. Sci. Technol.* 40 (2006) 67–73.
- [52] R.B. Neumann, K.N. Ashfaq, A.B. Badruzzaman, et al., Anthropogenic influences on groundwater arsenic concentrations in Bangladesh, *Nat. Geosci.* 3 (1) (2010) 46–52.
- [53] K. Yu, Y. Duan, Y. Gan, et al., Anthropogenic influences on dissolved organic matter transport in high arsenic groundwater: insights from stable carbon isotope analysis and electrospray ionization Fourier transform ion cyclotron resonance mass spectrometry, *Sci. Total Environ.* 708 (2020), 135162.
- [54] C. Yu, H. Guo, C. Zhang, et al., Variations and driving mechanism of dissolved arsenic in sediment porewater near wetland, *Appl. Geochem.* 137 (2022), 105185.
- [55] A.P. Tessier, P. Campbell, M.X. Bisson, Sequential extraction procedure for the speciation of particulate trace metals, *Anal. Chem.* 51 (7) (1979) 844–851.
- [56] H.A.L. Rowland, R.L. Pederick, D.A. Polya, et al., The control of organic matter on microbially mediated iron reduction and arsenic release in shallow alluvial aquifers, Cambodia, *Geobiology* 5 (2007) 281–292.
- [57] D.M. McKnight, E.W. Boyer, P.K. Westerhoff, et al., Spectrofluorometric characterization of dissolved organic matter for indication of precursor organic material and aromaticity, *Limnol. Oceanogr.* 46 (2001) 38–48.
- [58] J.E. Birdwell, A.S. Engel, Characterization of dissolved organic matter in cave and spring waters using UV-Vis absorbance and fluorescence spectroscopy, *Org. Geochem.* 14 (2010) 270–280.
- [59] A. Huguet, L. Vacher, S. Relexans, et al., Properties of fluorescent dissolved organic matter in the Gironde Estuary, *Org. Geochem.* 40 (2009) 706–719.
- [60] T. Ohno, Fluorescence inner-filtering correction for determining the humification index of dissolved organic matter, *Environ. Sci. Technol.* 36 (2002) 742–746.
- [61] J.L. Weishaar, G.R. Aiken, B.A. Bergamaschi, et al., Evaluation of specific ultraviolet absorbance as an indicator of the chemical composition and reactivity of dissolved organic carbon, *Environ. Sci. Technol.* 37 (20) (2003) 4702–4708.
- [62] H. Mori, F. Maruyama, H. Kato, et al., Design and experimental application of a novel non-degenerate universal primer set that amplifies prokaryotic 16S rRNA genes with a low possibility to amplify eukaryotic rRNA genes, *DNA Res.* 21 (2014) 217–227.
- [63] N. Xu, G.G. Tan, H.Y. Wang, et al., Effect of biochar additions to soil on nitrogen leaching, microbial biomass and bacterial community structure, *Eur. J. Soil Biol.* 74 (2016) 1–8.
- [64] E. Stackebrandt, B.M. Goebel, Taxonomic note: a place for DNA-DNA reassociation and 16S rRNA sequence analysis in the present species definition in bacteriology, *Int. J. Syst. Bacteriol.* 44 (1994) 846–849.
- [65] R.C. Edgar, UPARSE: highly accurate OTU sequences from microbial amplicon reads, *Nat. Methods* 10 (10) (2013) 996.
- [66] Q. Wang, G.M. Garrity, J.M. Tiedje, et al., Naïve Bayesian classifier for rapid assignment of rRNA sequences into the new bacterial taxonomy, *Appl. Environ. Microbiol.* 73 (2007) 5261–5267.
- [67] E. Pruesse, C. Quast, K. Knittel, et al., SILVA: a comprehensive online resource for quality checked and aligned ribosomal RNA sequence data compatible with ARB, *Nucleic Acids Res.* 35 (2007) 7188–7196.
- [68] C. Quast, E. Pruesse, P. Yilmaz, et al., The SILVA ribosomal RNA gene database project: improved data processing and web-based tools, *Nucleic Acids Res.* 41 (2013) 590–596.
- [69] M.L. Polizzotto, B.D. Kocar, S.G. Benner, et al., Near-surface wetland sediments as a source of arsenic release to ground water in Asia, *Nature* 454 (7203) (2008) 505–508.
- [70] N. Kumar, R.M. Couture, R. Millot, et al., Microbial sulfate reduction enhances Arsenic mobility downstream of zero valent iron based Permeable Reactive Barrier, *Environ. Sci. Technol.* 50 (14) (2016) 7610–7617.
- [71] N. Mladenov, Y. Zheng, B. Simone, et al., Dissolved organic matter quality in a shallow aquifer of Bangladesh: implications for arsenic mobility, *Environ. Sci. Technol.* 49 (2015a) 10815–10824.
- [72] A.D. Redman, D.L. Macalady, D. Ahmann, Natural organic matter affects arsenic speciation and sorption onto hematite, *Environ. Sci. Technol.* 36 (13) (2002) 2889–2896.
- [73] P. Sharma, M. Rolle, B. Kocar, et al., Influence of natural organic matter on arsenic transport and retention, *Environ. Sci. Technol.* 45 (2) (2011) 546–553.
- [74] M. Bauer, C. Blodau, Mobilization of arsenic by dissolved organic matter from iron oxides, soils and sediments, *Sci. Total Environ.* 354 (2) (2006) 179–190.
- [75] J. Wang, C.F. Kerl, P. Hu, et al., Thiolated arsenic species observed in rice paddy pore waters, *Nat. Geosci.* 321 (2020) 184.
- [76] V.S. Coker, A.G. Gault, C.I. Pearce, et al., XAS and XMCD evidence for species-dependent partitioning of arsenic during microbial reduction of ferrihydrite to magnetite, *Environ. Sci. Technol.* 40 (2006) 7745–7750.
- [77] J. Tang, X. Li, Y. Luo, et al., Spectroscopic characterization of dissolved organic matter derived from different biochars and their polycyclic aromatic hydrocarbons (PAHs) binding affinity, *Chemosphere* 152 (2016) 399–406.
- [78] F.S. Islam, A.G. Gault, C. Boothman, et al., Role of metal-reducing bacteria in arsenic release from Bengal delta sediments, *Nature* 430 (6995) (2004) 68–71.
- [79] S. Fendorf, H.A. Michael, A. van Geen, Spatial and temporal variations of groundwater arsenic in South and Southeast Asia, *Science* 328 (5982) (2010)

- 1123–1127.
- [80] R.B. Neumann, L.E. Pracht, M.L. Polizzotto, et al., Biodegradable organic carbon in sediments of an arsenic-contaminated aquifer in Bangladesh, *Environ. Sci. Technol. Lett.* 1 (4) (2014) 221–225.
- [81] M.A. Vega, H.V. Kulkarni, N. Mladenov, et al., Biogeochemical controls on the release and accumulation of Mn and as in shallow aquifers, West Bengal, India, *Front. Environ. Sci.* 5 (2017) 29.
- [82] O. Francioso, S. Sanchez-Cortes, V. Tugnoli, et al., Infrared, Raman, and nuclear magnetic resonance (¹H, ¹³C, and ³¹P) spectroscopy in the study of fractions of peat humic acids, *Appl. Spectrosc.* 50 (9) (1996) 1165–1174.
- [83] X. Qu, L. Xie, Y. Lin, et al., Quantitative and qualitative characteristics of dissolved organic matter from eight dominant aquatic macrophytes in Lake Dianchi, China, *Environ. Sci. Pollut. Control Ser.* 20 (10) (2013) 7413–7423.
- [84] T. Luo, H. Tian, Z. Guo, et al., Fate of arsenate adsorbed on Nano-TiO₂ in the presence of sulfate reducing bacteria, *Environ. Sci. Technol.* 47 (2013) 10939–10946.
- [85] Y.P. Yang, H.M. Zhang, H.Y. Yuan, et al., Microbe mediated arsenic release from iron minerals and arsenic methylation in rhizosphere controls arsenic fate in soil-rice system after straw incorporation, *Environ. Pollut.* 236 (2018) 598–608.
- [86] R.S. Oremland, J.F. Stolz, J.T. Hollibaugh, The microbial arsenic cycle in Mono Lake, California, *FEMS (Fed. Eur. Microbiol. Soc.) Microbiol. Ecol.* 48 (1) (2004) 15–27.
- [87] C. Lv, C. Zhao, S. Yang, Arsenic metabolism in purple nonsulfur bacteria, *Acta Microbiol. Sin.* 52 (12) (2012) 1497–1507.
- [88] D. Freikowski, J. Winter, C. Gallert, Hydrogen formation by an arsenate-reducing *Pseudomonas putida*, isolated from arsenic-contaminated groundwater in West Bengal, India, *Appl. Microbiol. Biotechnol.* 88 (6) (2010) 1363–1371.
- [89] M. Herbel, S. Fendorf, Biogeochemical processes controlling the speciation and transport of arsenic within iron coated sands, *Chem. Geol.* 228 (1–3) (2006) 16–32.
- [90] L. Cavalca, R. Zanchi, A. Corsini, et al., Arsenic-resistant bacteria associated with roots of the wild *Cirsium arvense* (L.) plant from an arsenic polluted soil, and screening of potential plant growth-promoting characteristics, *Syst. Appl. Microbiol.* 33 (3) (2010) 154–164.
- [91] V.H.C. Liao, Y.J. Chu, Y.C. Su, et al., Arsenite-oxidizing and arsenate-reducing bacteria associated with arsenic-rich groundwater in Taiwan, *J. Contam. Hydrol.* 123 (1) (2011) 20–29.
- [92] Y. Li, Characterization and Biogeochemical Functions of Indigenous Microbes in the Hetao Aquifer Systems, Inner Mongolia[D], China University of Geosciences (Beijing, 2016 (in Chinese with English abstract).
- [93] J. Akai, A. Kanekiyo, N. Hishida, et al., Biogeochemical characterization of bacterial assemblages in relation to release of arsenic from South East Asia (Bangladesh) sediments, *Appl. Geochem.* 23 (11) (2008) 3177–3186.
- [94] Y. Deng, T. Zheng, Y. Wang, et al., Effect of microbially mediated iron mineral transformation on temporal variation of arsenic in the Pleistocene aquifers of the central Yangtze River basin, *Sci. Total Environ.* 619–620 (2018) 1247–1258.
- [95] C.E. Lawson, B.J. Strachan, N.W. Hanson, et al., Rare taxa have potential to make metabolic contributions in enhanced biological phosphorus removal ecosystems, *Environ. Microbiol.* 17 (2015) 4979–4993.
- [96] W. Qiao, H.M. Guo, C. He, et al., Unraveling roles of dissolved organic matter in high arsenic groundwater based on molecular and optical signatures, *J. Hazard Mater.* 406 (2020b), 124702.
- [97] J. Jin, A.R. Zimmerman, S.B. Norton, et al., Arsenic release from Floridan Aquifer rock during incubations simulating aquifer storage and recovery operations, *Sci. Total Environ.* 551 (2016) 238–245.
- [98] Y. Duan, M.V. Schaefer, Y. Wang, et al., Experimental constraints on redox-induced arsenic release and retention from aquifer sediments in the central Yangtze River Basin, *Sci. Total Environ.* 649 (PT.1–1662) (2019) 629–639.
- [99] X. Meng, R.R. Dupont, D.L. Sorensen, et al., Arsenic solubilization and redistribution under anoxic conditions in three aquifer sediments from a basin-fill aquifer in Northern Utah: the role of natural organic carbon and carbonate minerals, *Appl. Geochem.* 66 (2016) 250–263.
- [100] E.C. Gillispie, E. Andujar, M.L. Polizzotto, Chemical controls on abiotic and biotic release of geogenic arsenic from Pleistocene aquifer sediments to groundwater, *Environ. Sci. J. Integr. Environ. Res.: Process. Impacts* 18 (8) (2016) 1090–1103.
- [101] Y.M. Deng, Y.X. Wang, T. Ma, et al., Speciation and enrichment of arsenic in strongly reducing shallow aquifers at western Hetao Plain, northern China, *Environ. Geol.* 56 (7) (2009) 1467–1477.
- [102] S. Sudarsan, S. Dipankar, Role of shallow alluvial stratigraphy and Holocene geomorphology on groundwater arsenic contamination in the Middle Ganga Plain, India, *Environ. Earth Sci.* 73 (7) (2015) 3523–3536.
- [103] Athena A. Nghiem, Stahl, O. Mason, Brian J. Mailloux, et al., Quantifying riverine recharge impacts on redox conditions and arsenic release in groundwater aquifers along the Red River, Vietnam, *Water Resour. Res.* 55 (8) (2019).
- [104] H. Neidhardt, Z.A. Berner, D. Freikowski, et al., Organic carbon induced mobilization of iron and manganese in a West Bengal aquifer and the muted response of groundwater arsenic concentrations, *Chem. Geol.* 367 (2014) 51–62.
- [105] Y. Wang, J.J. Jiao, J.A. Cherry, Occurrence and geochemical behavior of arsenic in a coastal aquifer-aquitard system of the Pearl River Delta, China, *Sci. Total Environ.* 427–428 (Jun.15) (2012) 286–297.
- [106] C.C. Liu, S. Kar, J.S. Jean, et al., Linking geochemical processes in mud volcanoes with arsenic mobilization driven by organic matter, *J. Hazard Mater.* 262 (Nov.15) (2013) 980–988.
- [107] X. Xie, Y. Wang, C. Su, Hydrochemical and sediment biomarker evidence of the impact of organic matter biodegradation on arsenic mobilization in shallow aquifers of Datong Basin, China, *Water, Air, Soil Pollut.* 223 (2) (2012) 483–498.
- [108] K. Kuroda, T. Hayashi, A. Funabiki, et al., Holocene estuarine sediments as a source of arsenic in Pleistocene groundwater in suburbs of Hanoi, Vietnam, *Hydrogeol. J.* 25 (4) (2017) 1137–1152.
- [109] Papacostas, C. Nicholas, Benjamin C. Bostick, Andrew N. Quicksall, et al., Geomorphic controls on groundwater arsenic distribution in the Mekong River Delta, Cambodia, *Geology* 36 (11) (2008) 891–894.
- [110] H.M. Anawar, J. Akai, K. Komaki, et al., Geochemical occurrence of arsenic in groundwater of Bangladesh: sources and mobilization processes, *J. Geochem. Explor.* 77 (2–3) (2003) 109–131.
- [111] A.J. Desbarats, T. Pal, P.K. Mukherjee, et al., Geochemical evolution of groundwater flowing through arsenic source sediments in an aquifer system of West Bengal, India, *Water Resour. Res.* 53 (11) (2017) 8715–8735.
- [112] S. Bavisakar, R. Choudhury, C. Mahanta, Dissolved and solid-phase arsenic fate in an arsenic-enriched aquifer in the river Brahmaputra alluvial plain, *Environ. Monit. Assess.* 187 (3) (2015) 1–14.
- [113] Z.M. Xie, Y.X. Wang, M.Y. Duan, et al., Arsenic release by indigenous bacteria *Bacillus cereus* from aquifer sediments at Datong Basin, northern China, *Front. Earth Sci.* 5 (1) (2011) 37–44.
- [114] M. HERY, B.E. VAN DONGEN, F. GILL, et al., Arsenic release and attenuation in low organic carbon aquifer sediments from West Bengal, *Geobiology* 8 (2) (2010) 155–168.
- [115] V.H.C. Liao, Y.J. Chu, Y.C. Su, et al., Assessing the mechanisms controlling the mobilization of arsenic in the arsenic contaminated shallow alluvial aquifer in the blackfoot disease endemic area, *J. Hazard Mater.* 197 (2011) 397–403.
- [116] B. Mohapatra, A. Saha, A.N. Chowdhury, et al., Geochemical, metagenomic, and physiological characterization of the multifaceted interaction between microbiome of an arsenic contaminated groundwater and aquifer sediment, *J. Hazard Mater.* (2021) 125099.
- [117] Y. Sun, J. Lan, X. Chen, et al., Impacts of external organic carbon on arsenic release in aquifer of Jiangnan Plain, Central China, *ACS Earth Space Chem.* 5 (6) (2021) 1343–1354.
- [118] J.E. Mclean, R.R. Dupont, D.L. Sorensen, Iron and arsenic release from aquifer solids in response to biostimulation, *J. Environ. Qual.* 35 (4) (2006).
- [119] J. Park, J. Lee, J.U. Lee, et al., Microbial effects on geochemical behavior of arsenic in As-contaminated sediments, *J. Geochem. Explor.* 88 (1) (2006) 134–138.
- [120] M. Duan, Z. Xie, Y. Wang, et al., Microcosm studies on iron and arsenic mobilization from aquifer sediments under different conditions of microbial activity and carbon source, *Environ. Geol.* 57 (5) (2009) 997.
- [121] H.M. Anawar, J. Akai, T. Yoshioka, et al., Mobilization of arsenic in groundwater of Bangladesh: evidence from an incubation study, *Environ. Geochem. Health* 28 (6) (2006) 553–565.
- [122] Z. Chen, G. Dong, L. Gong, et al., The role of low-molecular-weight organic carbons in facilitating the mobilization and biotransformation of as(V)/Fe(III) from a realgar tailing mine soil, *Geomicrobiol. J.* (2018) 1–9.
- [123] S. Bonneville, P. Van Cappellen, T. Behrends, Microbial reduction of iron(III) oxyhydroxides: effects of mineral solubility and availability, *Chem. Geol.* 212 (3–4) (2004) 255–268.
- [124] S. Glasauer, P.G. Weidler, S. Langley, et al., Controls on Fe reduction and mineral formation by a subsurface bacterium, *Geochem. Cosmochim. Acta* 67 (7) (2003) 1277–1288.
- [125] B.D. Kocar, T. Borch, S. Fendorf, Arsenic repartitioning during biogenic sulfidation and transformation of ferrihydrite, *Geochem. Cosmochim. Acta* 74 (3) (2010) 980–994.
- [126] D. Postma, F. Larsen, N.T.M. Hue, et al., Arsenic in groundwater of the Red River floodplain, Vietnam: controlling geochemical processes and reactive transport modeling, *Geochem. Cosmochim. Acta* 71 (21) (2007) 5054–5071.
- [127] D. Postma, S. Jessen, N.T.M. Hue, et al., Mobilization of arsenic and iron from Red River floodplain sediments, Vietnam, *Geochem. Cosmochim. Acta* 74 (12) (2010) 3367–3381.
- [128] Y. Duan, Y. Gan, Y. Wang, et al., Temporal variation of groundwater level and arsenic concentration at Jiangnan Plain, central China, *J. Geochem. Explor.* 149 (12) (2014) 106–119.
- [129] E.J. O'Loughlin, C.A. Gorski, M.M. Scherer, et al., Effects of oxyanions, natural organic matter, and bacterial cell numbers on the bioreduction of lepidocrocite (gamma-FeOOH) and the formation of secondary mineralization products, *Environ. Sci. Technol.* 44 (12) (2010) 4570–4576.
- [130] N.S. Malvankar, M. Vargas, K.P. Nevin, et al., Tunable metallic-like conductivity in microbial nanowire networks, *Nat. Nanotechnol.* 6 (9) (2011) 573–579.
- [131] X. Xie, A. Ellis, Y. Wang, et al., Geochemistry of redox-sensitive elements and sulfur isotopes in the high arsenic groundwater system of Datong Basin, China, *Sci. Total Environ.* 407 (12) (2009) 3823–3835.
- [132] M.L. Polizzotto, C.F. Harvey, G. Li, et al., Solid-phases and desorption processes of arsenic within Bangladesh sediments, *Chem. Geol.* 228 (1–3) (2006) 97–111.